PRELIMINARY INVESTIGATION OF THE MIXING
OF A PULSATING AIR JET
IN A STEADY SECONDARY AIRFLOW

A Thesis

Submitted to the Graduate Faculty

of the University of Minnesota

by

Charles J. Burton

Lt. Comdr., U.S. Navy

In Partial Fulfillment of the Requirements

for the Degree of

Master of Science in Aeronautical Engineering

August 1951

ACKNOWLEDGEMENTS

The author wishes to express thanks to Dr. Newman A. Hall and Professor Thomas E. Murphy for their academic aid and counsel, to the Navy group and Patricia Burton who kindly assisted in operating the equipment and taking data, and to Michael Shonberg, E. Kaar, and William Alden for valuable suggestions and material aid in construction of the test set-up.

Thanks are also due to the U.S. Naval Postgraduate School, Annapolis, Maryland, which sponsored the attendence of the author at the University of Minnesota as a candidate for the degree of Master of Science.

TABLE OF CONTENTS

Summary 1

Introduction 2

The Statement of the Problem 2

Basis of Solution of the Problem 4

The Apparatus 6

General Description of Complete Apparatus . . . 6

The Pressure Sampling Valve 8

The Pulsator 11

The Air Flow System 12

Instrumentation 13

Miscellaneous Apparatus 15

Test Procedure 17

Test of Serviceability and Accuracy of Apparatus 17

Tests of the Flow Mixing Region 19

Discussion of Results 21

The Operating Limits of the Sampling Valve . . 21

The Mixing Region Flow Data 24

Conclusions and Recommendations 35

Bibliography 39

Appendix 40

LIST OF TABLES

Table		
I to X	Pulsating Flow, Cycle of Dynamic Pressure	43-52
XI to XIV	Dynamic Pressure Profiles	53-56
XV to XIX	Lines of Constant $\frac{q-q_s}{q_o-q_s}$	57-61
XX	Centerline Values of Velocity	62
XXI to XXII	Normalized Velocity Profiles	63-64

SUMMARY

An investigation of the mixing region of a cool isothermal pulsating air jet in a steady secondary airstream at Reynolds number = 41,000, velocity ratio $\cong$ 0.5, primary velocity $\cong$ 200 fps, was conducted by means of a velocity survey of the region, utilizing a total head tube, static pressure orifice, and a sampling valve, which by rotation and synchronization with the pulse producing valve, applied a constant but different pressure differential to each one of 36 manometer tubes in succession, producing a standing wave of dynamic pressure of the pulse cycle.

The pulsating flow mixing region was compared to the mixing region of a steady flow jet of similar configuration and found to differ very slightly, if at all. The mixing region agreed closely with that defined by previous steady flow investigations.

The investigation was conducted under the auspices of the Mechanical and Aeronautical Engineering Departments of the University of Minnesota in partial fullfillment of the requirements for the degree of Master of Science.

INTRODUCTION

The Statement of the Problem

The mixing of fluid jet with surrounding fluid has been investigated analytically with experimental confirmation by numerous investigators for various configurations of flow, but has always been limited to the steady flow cases. Based on Prandtl's mixing length concept for turbulent flow (1) [as modified by Taylor (2)], Tollmien (3) and Kuethe (4) have produced and confirmed theoretical analyses, of the extent and nature of the turbulent mixing regions formed by free jets.

Two excellent summaries of isothermal and non isothermal air jet investigations are reports by Cleeves and Boelter (5), and by Shapiro and Forstall (6), the latter report offering useful empirical relations for the shape of the mixing region.

Unfortunately, the non-steady flow case in which there exist pulsations of a random nature, and even that case in which the pulsations are regular, have not lent themselves to analytical treatment. It is felt that statistical methods will soon be brought to bear on the subject with productive results, but it is also desirable that supplementary data be introduced by experimental investigations.

The design engineer of turbojet, ramjet or pulsejet engine combustion chambers is confronted with a need for design data concerning the mixing of fuel vapor and air under highly turbulent conditions, often times under conditions of regular pulsing flow as in the case of the pulse-jet engine, or when resonant conditions exist in the combustion chambers of other types of jet engines.

It has been found by Godsey and Young (7) that such conditions exist in a gas turbine combustion chamber as evidenced by observed flickering of the flame front position at frequencies in 6000 cps, 250 to 600 cps, and 25-60 cps regions. And Scurlock (8) concludes that rough burning is due to random fluctuations in the mass flow, caused by fluctuations in the pressure drop which are in turn caused by random fluctuations of the fraction burned in any cross-section; and that resonance or flutter occurs when the period of vibration is the resonant frequency of some part of the system.

It is felt that a study of the basic mixing problem is a necessary prelude to further studies involving actual combustion. It is the purpose of this investigation, then, to show the extent of the mixing region of a low frequency pulsating air jet in a steady secondary air flow by means of a velocity survey of the region.

Basis of Solution of the Problem

The approach to this phase of the problem is experimental in nature. The axial velocity field can be charted by making a survey of the mixing region with a total head tube and static pressure taps. The difficulties involved in measuring non- steady pressures can be overcome, if the pressure variation is periodic, by use of a sampling valve which presents an open passage to a particular manometer at one point in the pressure cycle only and at the same point each cycle. Assuming no leakage from the tube during the rest of the cycle, the particular tube then is subjected to a steady pressure rather than a varying one. Use of many tubes, each recording a different point in the cycle then produces a standing wave of the pressure pulsation.

Static pressure readings can be taken at the edge of the flow for all points within the flow at a particular cross-section. Prandtl (1) has shown and Tollmien (3) has confirmed that the static pressure is constant across the jet within very small limits.

Direct comparison of the mixing region of a pulsating jet and the mixing region of a steady jet of similar strength will provide a measure of the pulsation mixing region as well as

its relationship to the steady flow case, for this particular configuration.

[illegible]

THE APPARATUS

General Description of Complete Apparatus

A schematic diagram of the apparatus used is shown in Fig. 1. Photographs of the apparatus components are Fig. 3 to Fig. 10.

The apparatus consisted of an air supply system capable of furnishing air to two flow lines which divided the air supply for primary and secondary air flow and which contained standard A.S.M.E. square edge orifices with "radius" taps as described in Ref. (9) for measurement of the mass rate of flow in each flow line. The primary flow passed through 2" standard galvanized pipe to a rotating disc type butterfly valve, which served as the source of pulsations, from whence it was smoothly ~~reached~~ reduced down to a one inch inside diameter brass tube and ejected into the test section as a free jet. The butterfly valve was separated from the measuring orifice by a $2\frac{1}{2}$ ft. by 7 ft. cylindrical surge tank to prevent the pressure pulsations from traveling upstream to the orifice and affecting its accuracy.

The secondary flow passed through a six inch I.D. smooth black-iron pipe, which contained the measuring orifice, to a 22 inch by 35 inch steel drum which served as a plenum cham-

ber and which surrounded the primary flow exit line concentrically. The secondary flow was then exited from the drum into a square "bell" which had an entrance dimension of 11 x 11 inches and which tapered smoothly to the 6 3/16 inch square test section to permit smooth entrance of the secondary flow into the test section, surrounding and concentric to the primary air jet. Eighteen-mesh screen was placed 14 inches upstream in the flow to assist in getting isotropic small scale turbulence at the test section entrance.

The test section consisted of an 8 ft. long square duct constructed of angle iron reinforced, smooth $\frac{1}{2}$ in. plywood. One side of the duct was constructed to slide so that the total head tube and static orifice located in the sliding panel could be placed at any desired station, longitudinally, in the test section. The downstream end of the duct was open.

The total head tube and static orifice pressure leads were connected to a rotating sampling valve which was syncronized with the rotating butterfly valve so that a standing wave of total pressure minus static pressure could be produced on a bank of U-tube manometers.

ber and which surrounded the primary flow exit lies concentrically. The secondary flow was then exited from the drum into a square "bell" which had an entrance dimension of 11 x 11 inches and which tapered smoothly to the 6 7/16 inch square test section to permit smooth entrance of the secondary flow into the test section, surrounding and concentric to the primary air jet. Eighteen-mesh screen was placed 14 inches upstream in the flow to assist in getting isotropic small scale turbulence at the test section entrance.

The test section consisted of an 8 ft. long square duct constructed of angle iron reinforced, smooth ½ in. plywood. One side of the duct was constructed to slide so that the total head tube and static orifice located in the sliding panel could be placed at any desired station, longitudinally, in the test section. The downstream end of the duct was open.

The total head tube and static orifice pressure leads were connected to a rotating sampling valve which was synchronized with the rotating butterfly valve so that a standing wave of total pressure minus static pressure could be produced on a bank of U-tube manometers.

The Pressure Sampling Valve

It was desired to know the variation of velocity, and thus pressure, with time in the mixing region. Available for this purpose was a rotating pressure sampling valve, constructed by E. R. Becker for his Master's Thesis (10). A schematic diagram of the sampling valve is shown in Fig. 2 and photographs of the valve and its associated drive mechanism and manometer board in Fig. 2-b to Fig. 2-h.

As described in Ref. 10 and Ref. 11, the valve consists of a truncated cone shaped rotor (A) which rotates within an outer casing (B). Two circumferential grooves, (C) and (D), have been machined in the conical section. Drilled in the outer casing, so that they match up with the two grooves in the conical section, are two pressure taps, (E) and (F). The pressure leads from the total head tube and the static pressure orifice at the test section were attached to these taps. An L shaped passage (G) has been made in each of the outer lands of the conical section resulting in a single hole in the face of the land. Drilled in the outer casing are 72 holes, 36 equally spaced in each of the two rings. These are situated to line up with the holes in the lands of the inner rotor. The outer casing is restricted from rotating by the pin (H) which passes through a slot in the supporting base (I). The rotor is driven by a pully and the outer

casing is held up on the taper by a spring arrangement. The outer casing is six inches in diameter at its largest and is tapered to a 30° included angle. It is supported by a pair of bearings and pillow blocks which provide for easy disassembly of the valve.

The principle of operation of the valve is as follows. The pressure changes are transmitted through the connections in to the two circumferential grooves machined in the surface of the rotor and up through the L shaped passages drilled in the two outer lands. As the conical rotor rotates, the pair of holes in the lands pass each of the 36 pairs of holes in the outer casing in succession. Different pressures exist in the L shaped passages as each pair is passed, but if the rotor is in synchronization with the pulsation frequency, and the pulsation is regular, the same pressures will exist in the L shaped passages each time the holes in the rotor lands pass a particular pair of holes in the outer casing. Thus, if connections are made to a different U-tube manometer from each pair of holes in the outer casing which occupy the same circumferential position, the pressure difference as it occurs at the particular point in the cycle of pulsation will be registered. With each of the 36 pairs of holes connected to U-tube manometers arranged in a bank, a standing wave showing the Δp at each 10° increment of the pulse cycle will appear on the manometer bank. This assumes that (1) the

level of the fluid in manometers have a common reference level, (2) that no leakage occurs from a tube, between successive applications of the Δp to that tube, and (3) that no additional positive or negative pressure is produced by the dynamic effects of the valve rotation itself. As will be described later, item (2) is a source of error which can be reduced by rotating the valve at speeds greater than 200 rpm and item (3) is a source of marked error which only calibration can lessen in the valve's present configuration.

The valve was driven by a $\frac{1}{2}$ hp, 110 volt, 1750 rpm, AC electric motor through a system of two 6 inch variable speed pulleys. An 8 inch pulley on the shaft of the inner rotor of the valve combined with these two variable speed pulleys afforded a speed range of 120 to 370 rpm.

The Pulsator

The source of pulsations in the primary flow was provided by a 2 inch diameter disc type butterfly valve which rotated in the primary flow pipe. The valve completely closed the passage when closed, thus the air flow varied from zero to maximum. The butterfly valve was connected to the inner rotor shaft of the sampler by a flexible shaft and a 2:1 gear ratio. The reduction gear synchronized the sampler valve and butterfly valve since one revolution of the butterfly valve constituted two complete pressure variation cycles.

The frequency of pulsation was adjusted by the variable speed pulley system and was controlled during runs by use of a stroboscope to accurately attain and maintain the desired pulse frequency.

The Airflow System

The air supply used for the tests was obtained from a permanent installation located in the turbine test cell of the Mechanical Engineering Department. A gasoline powered Lycoming Model O-435-T air cooled Army tank engine, rated at 162 hp at 2800 rpm, drives a centrifugal compressor. The compressor is a 7.48:1 gear ratio supercharger taken from an Allison V-1710 aircraft engine. The speed of the blower can be accurately controlled by throttling the engine.

A standard A.S.M.E. square edged orifice is mounted upstream of the blower inlet to permit evaluation of the mass rate of flow through the blower and to permit accurate maintenance of a desired flow rate.

Instrumentation

The total pressure was measured by a 0.028 inch O.D. total head tube of the Kiel type, which has a venturi shield surrounding the tube tip to insure flow normal to the 0.017 inch I.D. tube opening. The pitot tube shaft was $\frac{1}{4}$ inches O.D. brass which was mounted in a $\frac{1}{2}$ inch thick plexiglass plate through a leakproof packing gland so that the probe could be moved laterally across the test section width. The plexiglass plate also contained a 1/8 inch diameter static orifice. The plate was mounted in the sliding wooden panel of the test section so that it could move up and down independent of and/or longitudinally, with the panel; thus, the probe could be positioned at any point in the whole test section duct as desired.

The pressure difference, Δp, between total pressure and static pressure was indicated on the U-tube manometer bank previously described.

The pressure drops across the square edged measuring orifices were measured with well type water-filled manometers. The pressure taps from the orifices were located in accordance with A.S.M.E. standards for "radius taps", Ref. (9), the upstream tap being located 1 diameter from the upstream face of the orifice and the downstream tap $\frac{1}{2}$ diameter from the downstream

face of the orifice. The static pressure holes were $\frac{1}{4}$ inch diameter and free of burrs and restrictions with slightly rounded edges.

The static pressure level at the upstream tap was measured on the same manometer used to measure the pressure drop by clamping the lead from the downstream tap and removing its other end from the manometer, causing the manometer to indicate gage pressure just upstream of the orifice.

The temperatures at the orifices were measured by iron-constantan thermocouples inserted in the flow upsteam of the orifices in accordance with A.S.M.E. Standards. Temperature readings were made on a Brown direct indicating potentiometer.

The orifices were made to A.S.M.E. Standards and were machined to an inside diameter of 1.008 inches and 4.002 inches for the 2 inch primary line and the 6 inch secondary lines respectively.

A check on the accuracy of the orifices was made possible by the insertion of a measuring orifice at the blower inlet, which permitted a measurement of the total mass flow to compare with the sum of the flows through the primary and secondary lines as indicated by the other two measuring orifices.

Miscellaneous Apparatus

Flow Pipes. The A.S.M.E. code on fluid measurement does not recognize the use of any pipe smaller than 2 inch I.D. Consequently, 2 inch Standard galvanized iron pipe was used for the primary flow line and 6 inch I.D. smooth rolled black iron tubing for the secondary flow.

Surge Tanks. In order to prevent pulsations from the primary flow from affecting the measuring orifice in that line, the orifice was placed in series between two 7 ft. by $2\frac{1}{2}$ ft. cylindrical tanks which served to damp out pulsations originated from either side of the valve.

Since the pressure variations in the secondary flow line, caused by the pulsations in the primary flow line, were much smaller compared to total flow, and since the secondary flow orifice had a diameter ratio of 66 2/3 per cent it was felt that less capacity was needed to insure steady flow at the secondary flow orifice. Therefore the only surge tank used was a 22 inch x 35 inch steel drum placed between the possible source of pulsations (the test section) and the orifice. This drum served the additional purpose of a stilling chamber to aid in establishing a smooth isotropic entrance flow into the test section.

Throttling Orifice. In order to build up the pressure level of the air supply to the primary line so that a greater range of air flow control might be obtained, an orifice with an area ratio of 66 2/3 per cent was placed in the six inch line just downstream of the take-off of the 2 inch line. Then just ahead of the 2 inch line entrance to the first surge tank a gate valve was inserted in the line to permit variations in the primary air flow velocity. No provision was made to control the secondary air flow except by variation of total flow through changes in blower speed.

The Pulsator. The source of pulsations in the primary flow was provided by a 2 inch diameter disc type butterfly valve which rotated in the primary flow pipe. The valve completely closed the passage when closed, thus the air flow varied from zero to maximum. The butterfly valve was connected to the sampler rotor shaft through a 1:2 gear ratio. The reduction gear synchronized the sampler valve and butterfly valve since one revolution of the butterfly valve constituted two complete pressure variation cycles.

The frequency of pulsation was adjusted by the variable speed pulley system and was controlled during runs by use of a stroboscope to accurately attain and maintain the desired pulse frequency.

TEST PROCEDURE

Test of Serviceability and Accuracy of Apparatus

After the equipment was assembled, all joints and pressure leads were checked for leaks. The sampling valve was disassembled, inspected, lubricated with a mixture of SAE 10 motor oil and "Molykote", a molybdenum sulfide dry lubricant, and reassembled. A spring pressure of a fixed amount (that pressure which gave a spring constant of $\frac{4\text{lb}}{.020\text{in.}} = 200\ \frac{\text{lb}}{\text{in.}}$) was applied and maintained for all tests.

Next the manometer bank connections were checked for leakage by applying a Δp across one air passage of the sampler valve and then rotating the valve ten degrees to close off that passage. Since the valve leaks only while rotating this gave a check on the pressure leads from the valve to the manometers and a check on the proper assembly of the valve.

The valve was then operated through its speed range to check for overheating or other malfunction.

Next, with the engine running the gate valve was adjusted to give the desired ratio of primary velocity to secondary velocity of about two to one, the primary and secondary flows

being about 200 fps and 100 fps, respectively. The system was checked again for leakage. The effectiveness of the surge tanks was then checked by varying pulsator rpm and noting the effect on the manometers connected to the steady flow sections. In the range of 200 to 300 rpm no evidence of pulsations reaching the steady flow section was noted.

The accuracy of the measuring orifices was checked by computing the flows in the primary and secondary lines and comparing their sums with that flow measured by the orifice at the blower intake. Good agreement was found.

The effect of the length of the tubing connecting the total head tube and the static orifice to the valve was checked by comparing the readings on the manometer board using two sets of pressure leads, one set with the connection as short as possible, the other with 50" leads. No difference was found for these two lengths, consequently the 50" length was used for all readings. This was expected, since the natural resonant frequency for a 50" tube with one end open is on the order of 4000 cycles per minute and is higher for shorter lengths. The tubing used was 3/16 ID, thus not so small as to introduce capillary or extreme friction and attenuation effects.

No drifting or pulsating of the water columns in the manometer bank was observed during any of the check runs.

Tests of the Flow Mixing Region

Before starting the test runs, the engine and valve were run until fully warmed up and running conditions were stabilized.

To expedite taking readings, a large sheet of paper was placed behind the tubes of the manometer bank and the water column heights marked with pencil. The equilibrium positions of the water columns was marked on each new sheet before the run.

To obtain and maintain the desired pulse frequency of 250 rpm, a stroboscopic tachometer was used. A revolution counter and stopwatch was used for initial setting of the strobotach control since its control dial was not calibrated to the desired degree of accuracy.

Control of the airflow was maintained by throttling the driving engine, using the pressure drop across the primary flow measuring orifice as a reference. This value could be maintained constant to within 0.2 in. of water with little difficulty.

The initial run was a calibration run, made with the sampler valve rotating at 250 rpm. For a series of known steady flow values of dynamic pressure, "q", (total pressure minus static pressure) ranging from 3 inches to 16 inches of water, water

levels for all tubes in the manometer bank were marked for each "q" value. Other calibrations were made later in the tests for the purpose of maintaining an accurate calibration of the valve.

The pulsating runs were then made by connecting the butterfly valve to the sampler valve and marking the water levels of the manometer bank tubes for each probe position. The traverse consisted of readings taken each 0.1 inch starting beyond the nozzle centerline and continued through the nozzle centerline position to a distance of 2.5 inches from the centerline. This was accomplished for a series of stations commencing at the nozzle exit and continued to a distance of 39 nozzle diameters downstream.

For comparison with the pulsating flow tests, similar traverses were made with the butterfly valve disconnected from the sampler valve and in the full open position. Here, two traverses were made. One was made at a primary mass flow identical with the primary mass flow existing during the pulsating runs, so that the average velocity from the nozzle should be the same in both conditions. The other traverse was made at an arbitrary value of flow such that the q at the nozzle centerline at the exit was the same as the q at the peak of the cycle of the pulsating runs.

DISSCUSSION OF RESULTS

The Operating Limits of the Sampling Valve

Wong (11) describes in some detail the limitations, capabilities, and idiosyncracies of the sampler valve. In brief, the major source of error is leakage across the valve which varies with the pressure differential applied across the valve, the direction in which the Δp is applied, the speed of rotation of the valve, and the spring pressure which holds the outer casing against the rotor.

The speed of rotation of the valve affects the leakage in several ways. First, it determines the temperature of the valve which varies the viscosity and sealing power of the lubrication film. This establishes an upper limit of about 300 rpm beyond which the valve overheats rapidly. Low valve speed permits excessive leakage by prolonging the time interval during which leakage from the valve can occur between the successive instants when a particular manometer tube is subjected to its particular Δp at its point in the cycle. This places a lower limit of about 200 rpm upon the valve. Most critical are the dynamic effects of rotation. The valve rotor is not supported independently of the outer casing but rather is supported in a manner similar to a journal bearing; and as in the case of such

a bearing, rotation builds up an air film between the rotor and casing and a circumferential pressure gradient is established which is a function of the speed of rotation.

The valve is thus seen to be very inflexible in its present configuration. However, by remaining within the limits dictated and by removing the maximum number of variables it is possible, by calibration, to remove most of the error. Consequently, for this test a constant spring pressure was applied, a constant rpm was used, the pressure leads were attached with the lower pressure always connected to the narrow end of the rotor, and the valve was calibrated for these particular test conditions by applying a series of known steady Δp values to the rotating valve and marking the readings of the manometer tubes. From these readings a set of calibration curves over the range of 3" to 16" of water were plotted and found to be almost linear, as indicated by Wong. Fig. 16 is a calibration curve included as an example. The other calibration curves are not included since they apply only to this very particular combination of test conditions.

It was found desirable to run all the actual flow tests during the same test period since the calibration of the valve changed from day to day as the amount and condition of lubricant and other factors changed. Check runs made on other days re-

quired that new calibrations be made.

The need for extreme care in controlling the operation of the sampler valve, i.e., the necessity for babying it, the necessity for continuous recalibration, and its inflexibility, greatly reduce the scope of any testing done with it. The latitude of possible test conditions is narrowed by these limitations and the time consumed in obtaining, reducing and rechecking data is enormous. Nevertheless, it seems to be capable of producing reproducible results within its limitations.

<u>The Mixing Region Flow Data</u>

For the purpose of definition, the nozzle exit is taken as the origin of coordinates used in plotting the data. The distance along the nozzle centerline is denoted by $\frac{x}{D}$, positive downstream, in noxxle diameters. The lateral distance from the nozzle centerline is $\frac{y}{D}$. Thus $\frac{y}{D} = 0.5$ is the boundary of the nozzle and $\frac{x}{D} = 0$ is the station at the nozzle exit.

The value of 250 rpm used in these tests was arbitrary, prescribed by the limitations of the sampler valve, it not being practicable in the preliminary investigation to consider the effects of pulse frequency as a parameter.

The form of the pulsation wave was not controlled. The butterfly valve produces a flow varying from zero to maximum, of a form somewhat similar to harmonic wave shape.

The data is plotted in terms of dynamic pressure, $q = p_o - p_s = \frac{1}{2}\frac{\rho u^2}{g_o}$. Since the quantity q is proportional to the square of the velocity, it shows pressure variations more distinctly than a velocity plot. Fig. 17 in the appendix is a conversion plot of q to velocity, at the test conditions. For a ratio of q values, as in Figs. 14 and 15, no conversion is needed since a velocity ratio equals the square root of its corresponding q ratio. Key velocities and velocity ratios are indicated

on most plots.

Fig. 3 to Fig. 12 are plots of the dynamic pressure versus manometer tube, which is, in effect, a standing wave of the dynamic pressure cycle produced by one cycle of the butterfly valve. The butterfly valve full-open position corresponded to that position of the sampler valve which indicated on tube number 27. However, the peak of the q cycle is seen to occur some 110° later in the cycle, at about tube 2. At 250 rpm, this corresponds to about 73 milliseconds delay between the production and recording of a particular value. The delay is a constant value since the standing wave showed no phase shifting but held its position very steadily. The complete cause of the delay value was not ascertained since it amounts to an average velocity between butterfly valve and sampler valve of $\frac{6.25 \text{ ft}}{.073 \text{ sec.}}$ = 86 ft/sec. This is much less than the velocity at which the changed ratio of p_o/p_s due to throttling might be expected to travel and very much less than the local velocity of sound, at which approximate speed small pressure variations would travel. A possible explanation is that the major portion of the phase difference was due to the nature of the production of the pulsations. It is possible that the peak velocity through the butterfly did not occur exactly at the full open position. If most of the reduction in mass flow occurred when the butterfly was within,

say, 30° of the closed position, then the minimum velocity would occur when the mass flow was at a low level and the flow area was increasing, as at the 45° to 55° position beyond the closed position. Similarly the peak velocity would occur when the mass flow was at a high level and the flow area being reduced, as at about the opposite part of the cycle. This would place the peak velocity at about 50° past the full open position of the butterfly, or about 100° past tube 27, i.e., at tube 1 of the sampler.

The important fact relating to this investigation was that the sampler measured a standing wave which did not drift or pulsate.

The wave form in the pulsating jet is seen to be fairly regular. The scatter of data points is less than was expected, and curves were plotted through the points where evidence of cyclic variations occured so that resonant vibrations, if any, or other cyclic irregularities might be discerned. However, no consistent evidence was found that sympathetic vibrations were introduced into the system as had been the case in the work of Becker and Wong.

At the trough of each wave there was evidence of rapid pressure irregularities which it is believed were associated with the flow through the valve when the valve was very near the actual

ago, 80° of the closed position, then the minimum velocity would occur when the mass flow was at a low level and the flow area was increasing, as at the 40° to 60° position beyond the closed position. Similarly the peak velocity would occur when the mass flow was at a high level and the flow area being reduced, as it would the opposite part of the cycle. This would place the peak velocity at about 80° past the full open position of the pulsejet, or about 100° past tube 2), i.e., at tube 4 of the sampling.

The important fact relating to this investigation was that the exhaust was not a standing wave which did not shift or pulsate.

The wave form in the pulsating jet is seen to be fairly regular. The number of data points is less than was expected, and curves were plotted through the points where extremes of cyclic variations occurred so that resonance vibrations, if any, or other cyclic irregularities might be discerned. However, no consistent evidence was found that appreciable vibrations were introduced into the cycle as has been the case in the work of Becker and Berg.

At the trough of each wave there was evidence of rapid pressure irregularities which it is believed were associated with the flow through the valve when the valve was very near its seat

closed position.

Pressure pulses were transmitted to the secondary flow region, even at station $\frac{x}{D} = 0$, causing a q variation which averaged 0.5 in. of water. This was transmitted to the secondary flow outside the jet mixing region as a variation in static pressure. To confirm this, cyclic measurements of $p_o - p_{atm}$ and $p_s - p_{atm}$ were made at $\frac{x}{D} = 0$. The value of $p_s - p_{atm}$ was found to vary from -0.23 in. H_2O to -0.68 in. H_2O, a total variation of 0.45 in. H_2O.

The Kiel tube would not have been a suitable instrument for total head measurements had the flow configuration been such that flow reversals occurred. The check mentioned in the previous paragraph showed that total pressure varied smoothly from a value of about 15 in. H_2O to a minimum of about 9 in. at the trough of the cycle, at the nozzle centerline at $\frac{x}{D} = 0$. The minimum was about 5.75 in. H_2O at the edge of the jet and about 3 in. H_2O in the secondary flow. At no time did it approach zero. Thus the possibility of flow reversal was discounted.

Curves for successive $\frac{x}{D}$ stations show that a slight phase shift seems to be occurring as the flow moves downstream. The peak of waves for station $\frac{x}{D} = 12$ and beyond occurs closer to tube 3 than tube 2.

Fig. 13 and Fig. 14 are cross-plots from points from tubes 2, 13, and 17 in the earlior curves and from the steady flow data. They are profiles of dynamic pressure showing the variation of q with $\frac{x}{D}$ and with $\frac{y}{D}$. The above mentioned tubes were chosen so as to have profiles of the peak, the minimum, and an intermediate portion of the cycle. That intermediate value was chosen which had a q_0 equal to that of the steady flow traverse which had been made with a primary mass flow equal to the primary mass flow of the pulsating flow. This permitted a direct comparison of a pulsating flow and a steady flow which had the same mass flow and same average velocities.

It is noted that due to the inability to control the secondary air flow and the fact that less blower speed was necessary in the steady flow case to produce identical mass flows for pulsating and for steady flows, the secondary flow was less for the steady flow case. However, the change was small, the ratio of secondary velocity to primary velocity being 0.45 in the steady flow case and 0.53 for pulsating flow, the ratio of 0.5 having been initially selected as the approximate value desired for this investigation.

Fig. 14 and Fig. 15 make it seem that the velocity profile of the jet at the nozzle exit was not very flat. However,

Fig. 15 and Fig. 16 are crossplots from points from tubes 6, 12, and 17 in the earlier curves and from the steady flow data. They are profiles of dynamic pressure showing the variation of q with $\frac{x}{D}$ and with $\frac{y}{D}$. The above mentioned values were chosen so as to form profiles of the peak, the minimum, and an intermediate portion of the cycle. That intermediate value was chosen which had a q_v equal to that of the steady flow intensity which was made with a primary mass flow equal to the primary mass flow of the pulsating flow. This permitted a direct comparison of a pulsating flow and a steady flow which had the same mass flow and mass average velocities.

It is noted that due to the inability to control the secondary air flow and the fact that some blower speed was necessary in the steady flow runs to produce identical mass flows for pulsating and for steady flows, the secondary flow was less for the steady flow runs. However, the effect was small, the ratio of secondary velocity to primary velocity being 0.42 in the steady flow runs and 0.45 for pulsating flows, the ratio of 0.5 having been initially selected as the approximate value desired for this investigation.

From Fig. 15 and Fig. 16 it is seen that the velocity profile of the jet at the nozzle exit was not very flat. However,

remembering that this a plot of q rather than velocity, one sees that the corresponding velocity profile would be much flatter. The edge velocity, if computed, is seen to be 75% of the maximum velocity, which is flatter than the so called laminar flow profile. Laminar flow was not desired in this test, and with the disturbance created by the butterfly and the existing Reynolds number of 41,000 the primary flow is distinctly turbulent.

The profiles show two things clearly, that a marked similarity exists between the pulsating and steady cases, the pulsating flow having a slightly flatter initial profile, and that the profile in each case shows signs of approaching the flat condition at about $\frac{x}{D} = 21$. At this station, the ratio of the maximum velocity to secondary velocity is:

	u_o/u_s
Pulsating, maximum	1.20
Pulsating, minimum	1.15
Pulsating, intermediate	1.12
Steady, intermediate	1.19

By station $\frac{x}{D} = 27.5$, the ratios had become:

	u_o/u_s
Pulsating, maximum	1.10
Pulsating, minimum	1.10
Pulsating, intermediate	1.06
Steady, intermediate	1.10

By station $\frac{x}{D} = 39$, in each case, the velocity profile was not apparent to the measuring equipment. This is not in ac-

cordance with the work of Shapiro and Forstall (6) who found that for steady flow a "slope coefficient", a measure of the normalized profile slope was constant as far downstream as 140 diameters. However, since velocity along the axis beyond the core of potential flow decreases with increasing $\frac{x}{D}$, more reliable and sensitive measuring equipment than the sampler valve will be necessary to carry the investigation further downstream than was done in this test.

Despite the fact that this investigation was fundamentally concerned with the direct comparison of a steady jet and a pulsating jet having identical configurations except for steadiness and non-steadiness, it was desired, for purposes of evaluating the type of steady flow actually attained and evaluating the accuracy of measurement, to compare the mixing region characteristics with those defined by previous investigations. One of the most useful presentations of experimental data and empirical relations for jet flows of the nature present in this investigation is that by Forstall and Shapiro (6). Among their findings are that:

(1) All normalized velocity (and concentration) profiles downstream of the core of potential flow have strikingly similar shapes which are substantially independent of $\frac{x}{D}$. Furthermore, these shapes may be represented rather well by several

mathematical expressions, a cosine curve being the most similar.

(2) Beyond the end of the potential core, the value of velocity (and concentration) varies inversely with x, irrespective of the velocity ratio, λ.

(3) Some empirical relations based on their experimental data are:

(a) The $\frac{x}{D}$ value for the end of the potential core:

$$L = 4 + 12 \lambda$$

(b) Velocity decay downstream of the potential core, $(\frac{x}{D} > L)$:

$$\frac{u-u_s}{u_o-u_s} = \frac{L}{\frac{x}{D}}$$

A comparison of the experimental data of this experiment with the above empirical relations is made in Fig. 14-c and Fig. 14-d. Very close agreement was obtained with the empirical rate of velocity decay, indicated by the 1:1 slope of the logarathmic plots. The exact actual position of the end of the potential core is of course indeterminable experimentally because a transition region exists rather than a sharp boundary, as indicated by the lack of a sharp break in the experimental plot. However, the approximate position can be found by continuing the straight line velocity plots to their intersections. This produces an "L" position about 1.5 diameters less than the em-

pirical value for the steady jet and about 2.5 diameters less for the pulsating jet. This is considered good agreement.

The velocity parameter $\frac{u-u_s}{u_o-u_s}$ was chosen to reduce all plots to the same scale, and to eliminate the effect of dissimilar secondary flows. This indicates the degree to which the jet retains its original excess of velocity over the secondary flow, a value of $\frac{u-u_s}{u_o-u_s} = 0$ thus indicating complete velocity mixing. A similar parameter was used for the q plots described later.

To compare shapes, the profiles were made dimensionless and normalized by plotting $\frac{u-u_s}{u_o-u_s}$ versus $\frac{r}{r_m}$. When fully normalized in this manner, the profiles (Fig. 14-e) at $\frac{x}{D} = 12$ and $\frac{x}{D} = 21$ (downstream of the potential core) are seen to be almost identical at both stations for the intermediate value steady and pulsed flows, except for a spreading near the base of the profile. Forstall and Shapiro, in their more carefully controlled experiment, encountered the spread to a lesser degree, it being caused by the poor experimental accuracy possible in determining $(u-u_s)$ near the edge of the jet.

Other profiles could not be checked because those at $\frac{x}{D}$ less than 12 were within the potential core and those at $\frac{x}{D}$ greater than 21 offered too few distinct points for a valid determination of r_m. However, these two profiles are considered

the most significant since the unnormalized velocity profiles differ markedly between the two stations, the profile at $\frac{x}{D}$ being that one at which definite flattening of the profile, is first observed.

For direct comparison, a cosine curve is also shown and gives good agreement in the region where experimental accuracy was good.

The previous comparisons then would indicate that the experimental accuracy of this investigation was better in the regions where larger pressure differentials being measured than near the edges of the jet where the pressure differentials were smaller. However, the good agreement of the data with that of previous investigators indicates that the accuracy of measurements was reasonably good.

To actually picture the jet mixing region, Fig. 15-a through Fig. 15-e were plotted. These plots delineate lines of constant q, utilizing the parameter $\frac{q-q_s}{q_o-q_s}$.

The following table, from values in Fig. 15, compares the points at which the centerline flow might be considered mixed to various degrees:

$\frac{x}{D}$ Values for Mixing 85%, 68% and 55% Completed:

	$\frac{u-u_s}{u_o-u_s}$		
	0.15	0.32	0.45
	x/D	x/D	x/D
Pulsating, maximum	35.0	24.5	19.0
Pulsating, minimum	37.0	27.0	18.3
Pulsating, intermediate	36.0	24.0	18.4
Steady, intermediate	35.0	21.0	17.1
Steady, maximum	34.0	23.0	16.0

From the above, the conclusion might be drawn that the steady flow mixes slightly more rapidly than the pulsating flow. However, the facts that the accuracy of the absolute levels of pressure measurement by the sampler value is not known, and that the measurements of the steady flow values are approximate to the extent that flow turbulence caused a manometer water level fluctuation of up to 0.5 inch of water would lead to a more reasonable conclusion that the velocity mixing in the steady flow case and the pulsating case differ in no appreciable degree, consistent with the control exercised in this investigation.

CONCLUSIONS AND RECOMMENDATIONS

With respect to the sampling valve, the conclusions to be drawn are:

1. It can be utilized in investigations of this nature in its present configuration, but at the cost of considerable time expended in calibration and rechecking of data.

2. The valve is extremely inflexible. Its range of operation could be extended and its accuracy increased by eliminating the bearing action of the rotor and by providing a means of cooling the rotor and casing.

3. When properly calibrated and used within its limitations it can provide reproducible data. However, the accuracy of the absolute level of pressure measurements is not definitely known, and the effects of pulsation form and frequency, and of the pressure differential applied across the vave, upon the accuracy of measurement could well be a subject of further investigation.

With respect to the test equipment, it is recommended that a more flexible, simpler design patterned after that of Forstall and Shapiro (6) in which the secondary flow is drawn through the test section rather than blown through would be adaptable to the turbine test cell layout of the Mechanical En-

gineering Department, and would provide for smoother flow entrance into the test section and permit more accurate determination of the velocity profile in the critical regions where mixing is almost complete.

The sampler valve must be redesigned, if possible, or a substitute method of measuring varying pressures be applied before tests beyond the scope of this preliminary investigation can be prosecuted to any degree of success.

In this investigation of the mixing of a pulsating air jet in a steady secondary airstream it was found that:

1. There was no appreciable difference between the velocity mix'ng region of a cool, isothermal pulsating jet and mixing region of a steady flow jet of similar configuration, at a Reynolds number of 41,000 and $\lambda = 0.5$, when pulsations were formed by regular interruption of the flow at 250 cpm.

2. There was good agreement with the findings of other investigations previously made for the steady flow case that:

(a) The fully normalized velocity profiles downstream of the potential core are of the same shape, irrespective of the value of $\frac{x}{D}$ and closely resemble a cosine curve.

(b) The centerline velocity, downstream of the

potential core, decays in direct proportion to the value of $\frac{x}{D}$.

(c) The location of the end of the potential core at the centerline is closely defined by the empirical relation

$$L = 4 + 12 \lambda$$

3. The close agreement of the data of this investigation in the region where pressure differences were large indicate a reasonably good level of accuracy. The inability to accurately define the outer edges of the jet, where the pressure differences are smaller indicate the need for more closely controlled pulsed flow investigations utilizing measuring equipment more sensitive than the mechanical sampling valve used in the experiment.

4. Based on the ratio of the jet velocity in excess of the secondary flow to the original jet velocity in excess of the secondary flow, $\frac{u-u_s}{u_o-u_s}$, the centerline flow was considered 85% mixed at an average $\frac{x}{D} = 36$ for both the steady and pulsating cases, was 68% mixed at an average $\frac{x}{D} = 24$, and was 45% mixed at an average $\frac{x}{D} = 18$. In both cases the steady flow jets appeared to mix slightly sooner than the pulsating jet, but the accuracy of the data does not justify drawing a firm conclusion to that effect.

5. It is recommended that further investigations of this nature be made to check the effects of variation in pulse frequency, of pulsation form, of velocity ratio, λ, and of Reynolds number, upon the nature of the mixing region of a pulsating jet.

It is believed that the use of high speed photography coupled with Schlieren and/or shadowgraph flow visualization techniques might prove a profitable avenue of investigation.

BIBLIOGRAPHY

(1) "Report on the Investigation of Developed Turbulence", L. Prandtl, N.A.C.A. T.M. #1231, September 1949.

(2) "The Transport of Vorticity and Heat Through Fluids in Turbulent Motion", G. I. Taylor, Proc. Roy. Soc. A135, p. 685 and 702, 1932.

(3) "Calculation of Turbulent Expansion Processes", Walter Tollmein, N.A.C.A. T.M. #1085, 1945.

(4) "Investigation of Turbulent Mixing Regions Formed by Jets", Arnold M. Kuethe, J.A.M., vol. 2, #3 pp. 87-95, September 1935.

(5) "Isothermal and Non-Isothermal Air Jet Investigations", V. Cleeves and L. M. K. Boelter, Chem. Eng. Prog., vol. 43, p. 123, March 1947.

(6) "Momentum and Mass Transfer in Coaxial Gas Jets", Walton Forstall, Jr. and A. H. Shapiro, Journal Applied Mechanics, vol. 17, No. 4, December 1950.

(7) "Gas Turbines for Aircraft", Godsey and Young, p. 152, McGraw-Hill, 1949.

(8) "Flame Stabilization and Propogation in High Velocity Gas Streams (100-400 fps)". A. C. Scurlock, MIT Guided Missile Program, Report #19, May 1948.

(9) Flow Measurement, 1949, A.S.M.E. Power Test Code 19.5; 4-1949.

(10) "The Relative Pressure Drop Coefficients for a Square Edged Orifice in Steady and Pulsating Flow", E. H. Becker, Master's Thesis, University of Minnesota, August 1950.

(11) "A Study of the Effect that Low Frequency Pulsations Have on Pressure Drop Coefficients for a Square Edged Orifice". Robert Y. Wong, Master's Thesis, University of Minnesota, August 1951.

(12) "The Effect of Pulsations on Flows of Gases", Horace Judd and D. B. Pheley, A.S.M.E. Trans., vol. 44, 1922.

APPENDIX

LIST OF SYMBOLS

Letters:

D Nozzle diameter, inches

L Axial distance from nozzle exit, in diameters, of end of potential core

p Pressure, psia or in. H_2O

q Dynamic pressure, psi or in. H_2O

r Radius, inches

r_m Radius, inches, where velocity is arithmetic average of secondary and centerline values at any x.

u Axial flow velocity at any point

x Axial distance from nozzle exit, inches

y Lateral distance from nozzle centerline, inches

Subscripts:

j Jet

o Total as in p_o; maximum as in q_o or u_o.

p Primary flow

s Static as in p_s; secondary flow as in q_s or u_s.

Greek Letters:

Δ Differential value

μ Absolute Viscosity $\frac{lb}{ft\text{-}sec}$

ρ Density, $\frac{lb}{ft^3}$

λ Ratio of secondary velocity to centerline velocity at $\frac{x}{D} = 0$.

1. Air Flow Measurement and Calculation

The orifices in the system have been installed in accordance with A.S.M.E. Code. The equation used to find the mass flow was:

$$W = 0.668\ A_2\ KEY\sqrt{\rho \Delta p}$$

where

W = Mass flow in lb per sec.

A_2 = Throat area in square in.

K = Flow coefficient

E = Area multiplier for thermal expansion of the orifice plate.

Y = Empirical expansion factor

ρ = Upstream density of flowing air

Δp = Pressure drop across the orifice plate in psi

For a typical example of the determination of the mass flow with an orifice plate, see Example 2, page 7, ref. (9).

Calculation of Reynolds Number

2. The Reynolds number was calculated from the following equation:

$$N_R = \frac{\rho u D}{\mu}$$

3. The natural frequency of the tube with one end closed is computed from the following equation:

$$f = \frac{a}{4L}$$

TABLE I

PULSATING FLOW

CYCLE OF DYNAMIC PRESSURE, q, IN INCHES OF WATER

$\frac{x}{D} = 0$

	$\frac{y}{D}$, Distance from Nozzle Center, inches						
Degrees	0	0.1	0.2	0.3	0.4	0.5	1.0 to 2.5
10	15.70	15.15	14.85	14.10	11.85	9.70	3.55
20	15.80	15.30	15.00	14.10	11.95	9.75	3.40
30	15.60	15.10	14.80	13.95	11.90	9.65	3.60
40	15.35	14.85	14.60	13.60	11.40	8.35	3.40
50	14.95	14.40	14.25	13.30	11.25	9.10	3.75
60	14.50	13.95	13.80	12.80	10.80	8.65	3.60
70	14.20	13.65	13.40	13.00	10.55	8.50	3.65
80	13.80	13.25	13.05	12.20	10.30	8.30	3.75
90	13.50	13.00	12.75	11.90	10.00	8.20	3.55
100	12.85	12.30	12.15	11.30	9.40	7.70	3.50
110	12.50	11.90	11.75	11.00	9.20	7.65	3.40
120	12.05	11.55	11.30	10.50	8.60	7.00	3.30
130	11.40	10.85	10.70	9.85	8.10	6.50	3.25
140	10.90	10.40	10.25	9.54	7.70	6.05	3.15
150	10.55	10.05	9.85	9.15	7.40	5.90	3.15
160	10.15	9.62	9.49	8.75	7.21	5.72	2.90
170	9.95	9.40	9.30	8.60	6.90	5.40	3.05
180	10.13	9.62	9.40	8.75	7.16	5.70	3.00
190	10.45	9.80	9.65	8.80	7.20	5.70	2.70
200	10,60	9.90	9.85	9.00	7.40	5.90	2.85
210	10.70	10.00	10.00	9.10	7.45	6.00	2.85
220	11.30	11.00	10.40	9.55	7.95	6.45	2.90
230	11.80	11.10	10.95	10.10	8.40	6.80	3.50
240	12.30	11.45	11.40	10.40	8.70	7.10	3.80
250	12.60	11.85	11.75	10.75	9.00	7.40	3.85
260	13.05	12.20	12.10	11.10	9.40	7.60	3.80
270	13.40	12.50	12.40	11.45	9.70	8.00	3.75
280	13.90	13.00	12.85	11.85	10.00	8.20	3.70
290	14.10	13.20	13.10	12.10	10.10	8.40	3.60
300	14.50	13.65	13.40	12.20	10.30	8.45	3.55
310	14.90	14.00	13.90	12.80	10.80	8.70	3.70
320	15.10	14.45	14.30	13.20	10.90	9.03	3.60
330	15.30	14.40	14.40	13.25	11.10	9.10	3.45
340	15.35	14.55	14.45	13.40	11.40	9.40	3.55
350	15.50	14.60	14.60	13.55	11.45	9.50	3.7
360	17.00	14.95	14.95	13.80	11.70	9.65	

TABLE II

PULSATING FLOW

CYCLE OF DYNAMIC PRESSURE, q, IN INCHES OF WATER

$\frac{x}{D} = 3$

	Distance from Nozzle Center, inches						
Degrees	0.0	0.2	0.3	0.4	0.5	0.6	0.7 to 2.5
10	15.20	14.50	13.25	10.75	7.10	4.00	3.45
20	15.45	14.75	13.40	10.90	7.05	4.05	3.50
30	15.40	14.70	13.25	10.80	7.05	4.00	3.50
40	15.05	14.35	12.95	10.50	6.90	3.90	3.50
50	14.70	14.00	12.55	10.25	6.65	3.85	3.50
60	14.30	13.60	12.30	9.85	6.45	3.85	3.50
70	14.00	13.70	11.90	9.60	6.30	3.85	3.50
80	13.45	12.75	11.50	9.45	6.20	3.85	3.50
90	13.10	12.40	10.90	9.20	6.05	3.80	3.50
100	12.70	12.00	10.75	8.65	5.80	3.60	3.40
110	12.30	11.60	10.15	8.45	5.55	3.50	3.25
120	11.85	11.15	10.00	8.05	5.35	3.40	3.25
130	11.15	10.50	9.55	7.80	5.10	3.25	3.05
140	10.80	10.00	9.25	7.60	5.00	3.25	3.10
150	10.35	9.70	8.70	7.25	4.80	3.05	2.95
160	10.00	9.30	8.55	7.15	4.70	3.00	2.95
170	9.70	9.10	8.20	6.85	4.60	3.15	3.00
180	10.00	9.20	8.40	7.10	4.70	3.50	3.40
190	10.15	9.45	8.35	6.95	4.65	3.45	3.30
200	10.20	9.50	8.30	6.85	4.55	3.50	3.20
210	10.35	9.65	8.45	6.90	4.55	3.55	3.10
220	10.60	9.90	8.65	7.15	4.80	3.50	3.25
230	11.05	10.35	9.10	7.60	5.00	3.50	3.40
240	11.65	10.95	9.55	8.00	5.30	3.50	3.30
250	11.80	11.10	9.90	8.15	5.45	3.65	3.45
260	12.35	11.65	10.30	8.55	5.65	3.70	3.50
270	12.70	12.00	10.55	8.75	5.85	3.75	3.50
280	12.90	12.20	10.80	9.05	5.93	3.80	3.45
290	13.40	12.60	11.35	9.35	6.15	3.80	3.50
300	13.80	13.10	11.50	9.40	6.25	3.85	3.45
310	14.10	13.40	11.90	9.80	6.40	3.85	3.50
320	14.30	13.60	12.00	10.05	6.40	3.80	3.45
330	14.50	13.80	12.55	10.25	6.60	3.85	3.50
340	14.80	14.10	12.70	10.35	6.55	3.80	3.50
350	14.90	14.20	12.80	10.60	6.75	3.85	3.50
360	15.10	14.40	12.90	10.65	6.80	3.85	3.45

TABLE III

PULSATING FLOW

CYCLE OF DYNAMIC PRESSURE, q, IN INCHES OF WATER

$\frac{x}{D} = 5$

Distance from Nozzle Center, inches

Degrees	0.0	0.1	0.2	0.3	0.4	0.5	0.8 to 2.5
10	14.10	13.60	12.60	9.95	7.50	5.00	3.45
20	14.25	13.85	12.70	10.00	7.50	5.05	3.50
30	14.20	13.75	12.65	9.95	7.50	5.20	3.60
40	13.90	13.35	12.30	9.70	7.25	4.95	3.45
50	13.60	13.10	12.05	9.50	7.10	4.95	3.55
60	13.20	12.65	11.60	9.10	6.70	4.80	3.55
70	13.00	12.35	11.40	9.00	6.65	4.75	3.60
80	12.60	12.15	11.20	8.85	6.65	4.80	3.70
90	12.30	11.80	10.90	8.60	6.50	4.70	3.55
100	11.70	11.30	10.30	8.15	6.15	4.40	3.33
110	11.35	11.00	10.10	8.05	6.25	4.25	3.25
120	11.00	10.60	10.55	7.60	5.65	4.10	3.20
130	10.35	10.00	9.10	7.05	5.20	4.02	3.10
140	10.00	9.65	8.80	6.70	5.00	3.90	3.10
150	9.70	9.30	8.55	6.55	4.80	3.69	3.00
160	9.32	8.95	8.21	6.45	4.70	3.40	3.00
170	9.00	8.60	7.90	6.10	4.45	3.28	2.95
180	9.25	8.95	8.30	6.50	5.10	3.50	3.00
190	9.10	8.70	7.90	6.10	4.61	3.50	3.00
200	9.25	8.85	8.00	6.30	4.80	3.59	3.00
210	9.40	8.95	8.10	6.30	4.80	3.42	2.79
220	9.94	9.51	8.62	6.85	5.25	3.80	3.06
230	10.35	10.00	9.05	7.20	5.40	4.10	3.31
240	10.70	10.25	9.30	7.40	5.60	4.20	3.30
250	11.15	10.75	9.75	7.70	5.85	4.20	3.49
260	11.45	11.05	10.05	8.05	6.20	4.50	3.50
270	11.90	11.40	10.30	8.25	6.35	4.70	3.61
280	12.30	11.75	10.65	8.50	6.50	4.80	3.50
290	12.45	11.90	10.80	8.60	6.45	4.75	3.51
300	12.80	12.25	11.10	8.70	6.60	4.85	3.50
310	13.25	12.75	11.50	9.10	6.75	4.90	3.56
320	13.40	12.95	11.75	9.25	6.96	5.05	3.60
330	13.65	13.05	12.00	9.40	7.00	5.00	3.55
340	13.85	13.15	12.20	9.70	7.25	5.10	3.60
350	13.90	13.25	12.30	9.80	7.45	5.20	3.60
360	13.90	13.35	12.35	9.80	7.50	5.10	3.48

TABLE IV

PULSATING FLOW

CYCLE OF DYNAMIC PRESSURE, q, IN INCHES OF WATER

$\frac{x}{D} = 9$

	Distance from Nozzle Center, inches					
Degrees	0.0	0.1	0.2	0.5	0.7	0.9 to 2.5
10	10.95	10.60	9.25	5.10	3.80	3.55
20	11.25	10.75	9.45	5.25	3.85	3.55
30	11.00	10.65	9.40	5.35	4.00	3.70
40	10.80	10.55	9.10	5.10	3.80	3.45
50	10.55	10.25	9.00	5.10	3.90	3.45
60	10.20	10.00	8.65	4.95	3.80	3.60
70	10.00	9.70	8.35	4.85	3.70	3.55
80	9.70	9.50	8.25	4.85	3.85	3.55
90	9.55	9.25	7.90	4.60	3.75	3.45
100	9.10	8.85	7.65	4.55	3.55	3.25
110	8.90	8.60	7.35	4.35	3.40	3.20
120	8.50	8.25	7.15	4.20	3.30	3.20
130	8.05	7.80	6.70	3.80	3.25	3.05
140	7.75	7.50	6.05	3.70	3.10	3.05
150	7.50	7.25	6.30	3.65	3.15	3.05
160	7.20	7.00	6.90	3.55	3.15	3.00
170	7.05	6.80	5.80	3.40	3.35	3.05
180	7.30	7.05	6.00	3.72	3.35	2.95
190	6.55	6.35	5.35	3.60	3.30	3.05
200	7.15	6.95	5.95	3.75	3.20	2.95
210	7.25	7.05	6.05	3.80	3.25	3.05
220	7.55	7.30	6.35	3.90	3.35	3.25
230	8.05	7.80	6.75	4.10	3.45	3.35
240	8.30	8.05	7.00	4.25	3.60	3.40
250	8.55	8.35	7.25	4.50	3.75	3.45
260	8.85	8.65	7.45	4.50	3.65	3.55
270	9.10	8.95	7.80	4.70	3.80	3.55
280	9.35	9.20	7.95	4.80	3.95	3.50
290	9.50	9.35	8.05	4.85	3.85	3.45
300	9.90	9.60	8.30	4.85	4.00	3.55
310	10.25	9.85	8.50	4.95	4.10	4.70
320	10.40	10.30	8.90	5.10	4.15	4.45
330	10.55	10.30	8.95	5.25	4.10	3.50
340	10.65	10.45	9.10	5.30	4.15	3.55
350	10.85	10.50	9.20	5.30	4.15	3.55
360	10.90	10.65	9.30	5.25	4.20	3.55

TABLE V

PULSATING FLOW

CYCLE OF DYNAMIC PRESSURE, q, IN INCHES OF WATER

$\frac{x}{D} = 12$

Distance from Nozzle Center inches

Degrees	0.0	0.1	0.2	0.3	0.5	0.7	0.9	1.1 to 2.5
10	8.20	8.05	7.95	6.95	5.80	4.65	4.05	3.60
20	8.20	8.10	7.90	6.95	5.80	4.65	4.00	3.60
30	8.30	8.15	7.90	7.00	5.95	4.65	4.05	3.65
40	8.11	7.95	7.70	6.85	5.75	4.50	4.00	3.60
50	7.85	7.70	7.70	6.65	5.65	4.50	3.90	3.60
60	7.90	7.80	7.50	6.60	5.60	4.55	4.05	3.70
70	7.60	7.40	7.20	6.35	5.55	4.35	3.95	3.60
80	7.60	7.35	7.50	6.15	5.55	5.00	4.00	3.65
90	7.20	7.00	6.72	6.09	5.22	4.30	3.90	3.50
100	7.00	6.80	6.55	5.80	5.15	4.06	3.68	3.40
110	6.75	6.50	6.40	5.65	4.90	4.05	3.60	3.30
120	6.50	6.30	6.10	5.50	4.75	3.90	3.53	3.30
130	6.35	6.10	5.90	5.35	4.60	3.75	3.50	3.20
140	6.10	5.85	5.85	5.12	4.41	3.70	3.44	3.20
150	5.90	5.75	5.40	5.00	4.32	3.52	3.30	3.00
160	5.66	5.00	5.15	4.85	4.25	3.50	3.25	3.00
170	5.31	5.10	4.75	4.51	3.96	3.40	3.10	2.90
180	5.60	5.40	5.07	4.75	4.20	3.50	3.25	3.00
190	5.40	5.20	4.90	4.60	4.10	4.10	3.20	2.95
200	5.50	5.25	5.00	4.69	4.20	3.53	3.25	2.90
210	5.50	5.25	5.15	4.80	4.30	3.40	3.23	3.00
220	5.80	5.68	5.35	5.00	4.40	3.71	3.30	3.10
230	6.10	5.90	5.70	5.15	4.55	3.85	3.50	3.20
240	6.27	6.02	5.88	5.25	4.60	3.90	3.59	3.30
250	6.70	6.40	6.20	5.60	4.90	4.11	3.70	3.45
260	6.85	6.65	6.35	5.75	5.10	4.20	3.80	3.55
270	7.00	6.85	6.65	5.95	5.20	4.30	3.90	3.60
280	7.15	6.95	6.75	6.00	5.35	4.40	3.90	3.60
290	7.30	7.10	6.95	6.15	5.40	4.45	3.91	3.60
300	7.50	7.30	7.05	6.30	5.45	4.40	3.90	3.50
310	7.75	7.50	7.30	6.40	5.60	4.40	3.85	3.50
320	7.73	7.60	7.34	6.50	5.55	4.40	3.90	3.50
330	8.00	7.65	7.50	6.70	5.70	4.35	3.95	3.55
340	8.15	7.95	7.70	6.70	5.70	4.50	3.95	3.60
350	8.13	7.95	7.70	6.80	5.85	4.60	4.00	3.55
360	8.25	8.05	7.90	6.90	5.95	4.55	4.02	3.60

TABLE VI

PULSATING FLOW

CYCLE OF DYNAMIC PRESSURE, q, IN INCHES OF WATER

$\frac{x}{D} = 21$

	Distance from Nozzle Center, inches				
Degrees	0.0	0.8	1.2	1.3	1.5 to 2.5
10	5.02	4.50	4.00	3.80	3.60
20	5.18	4.65	4.15	3.95	3.65
30	5.23	4.70	4.20	4.00	3.70
40	5.02	4.65	4.15	3.95	3.50
50	4.95	4.50	4.10	3.90	3.50
60	5.00	4.50	4.10	3.90	3.70
70	4.85	4.40	4.00	3.80	3.65
80	4.80	4.25	3.85	3.75	3.75
90	4.70	4.15	3.85	3.75	3.65
100	4.47	4.05	3.75	3.75	3.45
110	4.30	3.95	3.65	3.55	3.50
120	4.25	3.85	3.55	3.45	3.40
130	4.20	3.85	3.55	3.45	3.35
140	4.15	3.75	3.45	3.35	3.30
150	4.1	3.75	3.45	3.35	3.30
160	4.0	3.60	3.40	3.30	3.20
170	3.95	3.60	3.30	3.10	3.10
180	4.05	3.50	3.40	3.30	3.30
190	3.95	3.40	3.30	3.20	3.20
200	3.85	3.60	3.40	3.30	3.10
210	4.05	3.40	3.30	3.20	3.20
220	4.15	3.40	3.40	3.30	3.50
230	4.2	3.50	3.30	3.20	3.20
240	4.05	3.75	3.50	3.40	3.40
250	4.20	3.75	3.60	3.50	3.50
260	4.40	3.75	3.75	3.65	3.55
270	4.65	4.00	3.75	3.65	3.65
280	4.65	4.10	3.80	3.70	3.50
290	4.75	4.30	4.00	3.80	3.65
300	4.80	4.40	4.00	3.80	3.50
310	4.95	4.55	4.05	3.85	3.70
320	4.90	4.50	4.10	3.90	3.50
330	4.95	4.45	4.05	3.85	3.65
340	5.08	4.55	4.15	3.95	3.55
350	5.18	4.70	4.20	4.00	3.70
360	5.18	4.70	4.20	4.00	3.50

TABLE VII

PULSATING FLOW

CYCLE OF DYNAMIC PRESSURE, q, IN INCHES OF WATER

$\frac{x}{D} = 24\frac{1}{2}$

Distance from Nozzle Center, inches

Degrees	0.0 0.2	0.4	0.8	1.0	1.4	1.6 to 2.5
10	4.75	4.50	4.30	3.95	3.70	3.65
20	4.75	4.60	4.20	4.05	3.75	3.65
30	4.70	4.50	4.20	3.95	3.75	3.55
40	4.60	4.35	4.00	3.85	3.70	3.45
50	4.70	4.50	4.10	4.05	3.85	3.60
60	4.80	4.60	4.20	4.05	3.90	3.75
70	4.80	4.60	4.20	4.20	4.00	3.75
80	4.75	4.55	4.20	4.10	3.90	3.75
90	4.50	4.25	4.05	4.05	3.85	3.65
100	4.35	4.20	3.85	3.85	3.65	3.45
110	4.25	4.20	3.90	3.90	3.75	3.55
120	4.15	4.15	3.75	3.75	3.55	3.35
130	4.15	4.10	3.75	3.65	3.55	3.40
140	4.10	4.05	3.70	3.65	3.45	3.25
150	4.00	4.00	3.65	3.65	3.45	3.25
160	3.9	3.95	3.45	3.65	3.40	3.25
170	3.90	3.85	3.55	3.50	3.20	3.20
180	4.00	3.90	3.40	3.50	3.40	3.15
190	3.90	3.85	3.30	3.50	3.40	3.15
200	3.80	3.70	3.30	3.50	3.40	3.15
210	4.00	3.80	3.55	3.50	3.50	3.15
220	4.10	3.95	3.75	3.70	3.60	3.25
230	4.15	3.85	3.55	3.55	3.45	3.20
240	4.0	3.95	3.65	3.65	3.55	3.25
250	4.15	4.20	3.85	3.80	3.65	3.40
260	4.30	4.20	3.95	3.90	3.75	3.50
270	4.50	4.25	3.95	3.90	3.75	3.50
280	4.40	4.20	3.85	3.80	3.70	3.45
290	4.55	4.25	4.00	3.95	3.80	3.55
300	4.05	3.85	4.05	4.00	3.90	3.60
310	4.60	4.35	4.20	4.05	3.90	3.65
320	4.65	4.40	4.05	4.00	3.95	3.60
330	4.60	4.25	4.10	4.00	3.80	3.60
340	4.65	4.40	4.05	4.00	3.80	3.60
350	4.70	4.50	4.20	4.05	3.85	3.75
360	4.75	4.55	4.25	4.15	3.75	3.75

TABLE VIII

PULSATING FLOW

CYCLE OF DYNAMIC PRESSURE , q, IN INCHES OF WATER

$\frac{x}{D} = 27\frac{1}{2}$

	Distance from Nozzle Center, inches			
Degree	0.0 0.2 0.4	0.9	1.5	1.7 to 2.5
10	4.25	3.85	3.80	3.70
20	4.40	4.00	3.85	3.75
30	4.25	3.85	3.75	3.60
40	4.15	3.75	3.65	3.55
50	4.25	3.85	3.75	3.70
60	4.40	4.00	3.90	3.80
70	4.40	4.00	3.90	3.85
80	4.30	4.00	3.90	3.80
90	4.05	3.75	3.65	3.75
100	3.95	3.75	3.65	3.55
110	3.95	3.75	3.65	3.50
120	3.85	3.75	3.65	3.40
130	3.85	3.70	3.60	3.40
140	3.75	3.65	3.55	3.30
150	3.70	3.65	3.55	3.30
160	3.70	3.60	3.50	3.30
170	3.70	3.60	3.50	3.20
180	3.60	3.50	3.40	3.20
190	3.50	3.40	3.30	3.20
200	3.35	3.25	3.15	3.20
210	3.55	3.45	3.35	3.20
220	3.75	3.65	3.55	3.40
230	3.70	3.60	3.50	3.25
240	3.75	3.60	3.50	3.30
250	3.95	3.75	3.65	3.50
260	4.00	3.80	3.70	3.60
270	4.05	3.85	3.75	3.60
280	4.00	3.80	3.70	3.50
290	4.05	3.85	3.75	3.60
300	3.60	3.40	3.30	3.70
310	4.20	3.90	3.80	3.75
320	4.20	3.90	3.80	3.70
330	4.10	3.80	3.70	3.70
340	4.20	3.80	3.70	3.70
350	4.30	3.90	3.80	3.75
360	4.30	3.90	3.80	3.75

TABLE IX

PULSATING FLOW

CYCLE OF DYNAMIC PRESSURE, q, IN INCHES OF WATER

$\frac{x}{D} = 30$

	Distance from Nozzle Center, inches			
Degree	0.0 0.2 0.4	0.7	1.3	1.8 to 2.5
10	4.25	4.05	3.85	3.70
20	4.20	4.00	3.80	3.75
30	4.20	4.00	3.80	3.60
40	4.00	3.80	3.70	3.55
50	4.05	3.85	3.75	3.70
60	4.15	3.95	3.85	3.80
70	4.20	4.00	3.90	3.85
80	4.20	4.00	3.90	3.80
90	4.05	3.85	3.75	3.75
100	3.85	3.75	3.65	3.55
110	3.90	3.80	3.70	3.55
120	3.75	3.65	3.55	3.40
130	3.75	3.65	3.55	3.40
140	3.70	3.60	3.50	3.30
150	3.60	3.60	3.50	3.30
160	3.50	3.50	3.45	3.30
170	3.55	3.50	3.40	3.20
180	3.40	3.35	3.30	3.20
190	3.30	3.25	3.20	3.20
200	3.30	3.25	3.20	3.20
210	3.55	3.45	3.35	3.20
220	3.75	3.65	3.55	3.40
230	3.55	3.45	3.35	3.25
240	3.60	3.50	3.40	3.30
250	3.85	3.70	3.60	3.50
260	3.95	3.85	3.75	3.60
270	3.95	3.85	3.75	3.60
280	3.85	3.75	3.70	3.50
290	4.00	3.90	3.80	3.60
300	4.05	3.95	3.75	3.70
310	4.15	3.95	3.75	3.75
320	4.05	3.90	3.70	3.70
330	4.10	3.90	3.75	3.70
340	4.05	3.95	3.75	3.70
350	4.20	4.00	3.80	3.75
360	4.25	4.05	3.80	3.75

TABLE X

PULSATING FLOW

CYCLE OF DYNAMIC PRESSURE, q, IN INCHES OF WATER

$\frac{x}{D} = 39$

Degree	
10	3.70
20	3.75
30	3.60
40	3.55
50	3.70
60	3.80
70	3.85
80	3.80
90	3.75
100	3.55
110	3.60
120	3.50
130	3.40
140	3.30
150	3.30
160	3.30
170	3.20
180	3.20
190	3.20
200	3.20
210	3.20
220	3.40
230	3.25
240	3.30
250	3.50
260	3.60
270	3.60
280	3.50
290	3.60
300	3.70
310	3.75
320	3.70
330	3.70
340	3.70
350	3.75
360	3.75

TABLE XI

MAXIMUM DYNAMIC PRESSURE PROFILE

q, INCHES OF WATER

Pulsating Jet

$\frac{y}{D}$	$\frac{x}{D}$=0	3	5	9	12	21	24.5	27.5	30	39
0	15.8	15.45	14.25	11.25	8.3	5.2	4.75	4.4	4.2	3.75
.1	15.3		13.85	10.75	8.1		4.75	4.4		3.75
.2	15.	14.75	12.7	9.25	7.9			4.4	4.2	3.75
.3	14.1	13.40	10.0		6.95					3.75
.4	11.95	10.9	7.5				4.6	4.4	4.2	3.75
.5	9.75	7.05	5.05	5.25	5.8					3.75
.6		4.05	3.60							3.75
.7		3.5		3.85	4.65				4.0	3.75
.8		3.5	3.5			4.65	4.2			3.75
.9		3.5	3.5	3.55	4.0			4.0		3.75
1.0	3.4	3.5	3.5	3.55	3.75		4.05			3.75
1.1	3.4	3.5	3.5	3.55	3.6					3.75
1.2	3.4	3.5	3.5	3.55	3.6	4.15				3.75
1.3	3.4	3.5	3.5	3.55	3.6	3.95			3.8	3.75
1.4	3.4	3.5	3.5	3.55	3.6		3.75			3.75
1.5	3.4	3.5	3.5	3.55	3.6	3.65		3.8		3.75
1.6	3.4	3.5	3.5	3.55	3.6	3.65	3.65			3.75
1.7	3.4	3.5	3.5	3.55	3.6	3.65		3.75		3.75
1.8	3.4	3.5	3.5	3.55	3.6	3.65	3.65	3.75	3.75	3.75
2.5	3.4	3.5	3.5	3.55	3.6	3.65	3.65	3.75	3.75	3.75

TABLE XII

MINIMUM DYNAMIC PRESSURE PROFILE

q, INCHES OF WATER

Pulsating Jet

$\frac{y}{D}$	$\frac{x}{D}$ = 0	3	5	9	12	21	24.5	27.5	30
0	9.95	9.70	9.0	7.05	5.31	3.95	3.90	3.7	3.55
0.1	9.4		8.6	6.8	5.1				
0.2	9.3	9.10	7.9	5.8	4.75			3.7	
0.3	8.6	8.20	6.1		4.51				
0.4	6.9	6.35	4.45		3.96		3.85	3.7	
0.5	5.4	4.6	3.23	3.4					
0.6		3.15							
0.7		3.00		3.15	3.4				3.5
0.8		3.00	2.95			3.6	3.55		
0.9		3.00	2.95	3.05	3.1			3.6	
1.0	3.05	3.00	2.95	3.05			3.50		
1.1	3.05	3.00	2.95	3.05	2.9				
1.2	3.05	3.00	2.95	3.05	2.9	3.3			
1.3	3.05	3.00	2.95	3.05	2.9	3.1			3.4
1.4	3.05	3.00	2.95	3.05	2.9	3.1	3.2	3.5	
1.5	3.05	3.00	2.95	3.05	2.9	3.1	3.2		
1.6	3.05	3.00	2.95	3.05	2.9	3.1	3.2		
1.7	3.05	3.00	2.95	3.05	2.9	3.1	3.2	3.2	
1.8	3.05	3.00	2.95	3.05	2.9	3.1	3.2	3.2	3.2
2.5	3.05	3.00	2.95	3.05	2.9	3.1	3.2	3.2	3.2

TABLE XIII

INTERMEDIATE DYNAMIC PRESSURE PROFILE

q, INCHES OF WATER

Pulsating Jet

$\frac{y}{D}$ \ $\frac{x}{D}$	0	3	5	9	12	21	24.5	27.5	30	39
0	11.4	11.15	10.35	8.05	6.35	4.20	4.15	3.85	3.75	3.4
0.1	10.85		10.0	7.8	6.1					3.4
0.2	10.7	10.5	9.1	6.7	5.9		4.15			3.4
0.3	9.85	9.55	7.05		5.35					3.4
0.4	8.10	7.8	5.20				4.10	3.85	3.75	3.4
0.5	6.50	5.10	4.02	3.8	4.60					3.4
0.6	3.25	3.25								3.4
0.7	3.25	3.20		3.4	3.75				3.65	3.4
0.8	3.25	3.20	3.20			3.85	3.75			3.4
0.9	3.25	3.20	3.20	3.25	3.50			3.7		3.4
1.0	3.25	3.20	3.20	3.25			3.65			3.4
1.1	3.25	3.20	3.20	3.25	3.20					3.4
1.2	3.25	3.20	3.20	3.25	3.20	3.55				3.4
1.3	3.25	3.20	3.20	3.25	3.20	3.45			3.55	3.4
1.4	3.25	3.20	3.20	3.25	3.20		3.55			3.4
1.5	3.25	3.20	3.20	3.25	3.20	3.35		3.6		3.4
1.6	3.25	3.20	3.20	3.25	3.20	3.35	3.4			3.4
1.7	3.25	3.20	3.20	3.25	3.20	3.35	3.4	3.4		3.4
1.8	3.25	3.20	3.20	3.25	3.20	3.35	3.4	3.4	3.4	3.4

TABLE XIV

DYNAMIC PRESSURE PROFILE

Steady Flow - Intermediate Value

q, inches of water

$\frac{y}{D}$ \ $\frac{x}{D}$	0	3	5	9	12	16	21	24.5	27.5	30
0	11.4	10.7	10.3	7.6	5.9	4.3	3.4	3.2	2.95	2.9
0.1	11.3	10.6	9.8	7.3	5.9	4.2	3.4	3.15	2.95	2.9
0.2	10.7	10.2	8.5		5.4	4.2	3.35	3.10	2.9	2.9
0.3	9.4	9.1	6.2	6.2	4.6	4.1	3.2	3.1	2.9	2.85
0.4	7.1	6.1	4.6	4.8	4.2	3.9	3.1	3.0	2.9	2.7
0.5	5.9	3.7	2.9	3.9	3.5	3.4	3.0	2.95	2.85	2.65
0.6	2.3	2.5	2.4	3.4	3.0	3.2	2.9	2.90	2.8	2.6
0.7	2.2	2.3	2.3	2.9		3.0		2.85	2.75	2.6
0.8	2.2	2.3	2.3	2.6	2.7	2.9	2.7	2.8	2.7	2.6
0.9	2.3	2.3	2.3	2.5	2.6	2.7	2.7	2.7	2.7	2.6
1.0	2.3	2.3	2.3	2.4	2.5	2.6	2.6	2.6	2.6	2.6
1.1	2.3	2.3	2.3	2.4	2.4	2.6	2.55	2.55	2.6	2.5
1.2	2.3	2.3	2.3	2.4	2.4	2.5	2.5	2.45	2.55	2.45
1.3	2.3	2.3	2.3	2.4	2.4	2.5	2.4	2.4	2.5	2.45
1.4	2.3	2.3	2.3	2.4	2.4	2.4	2.4	2.4	2.45	2.45
1.5	2.3	2.3	2.3	2.4	2.4	2.4	2.4	2.4	2.4	2.45
1.6	2.3	2.3	2.3	2.4	2.4	2.4	2.4	2.4	2.4	2.45
2.0	2.3	2.3	2.3	2.4	2.4	2.4	2.4	2.4	2.4	2.45

TABLE XV

Lines of Constant $\frac{q-q_s}{q_o-q_s}$

Maximum Value, Pulsating Flow

$\frac{X'}{D}$ \ $\frac{Y'}{D}$ =	.037	.1	.2	.3	.4	.5	.6	.7	.8	.9
0							.45	.40	.36	.28
3	.58	.54	.51	.49	.45	.42	.39	.38	.30	.22
5	.60	.52	.46	.40	.35	.31	.26	.21	.15	
9	.65	.53	.39	.35	.26	.18	.08			
12	.90	.68	.50	.39						
21	1.22	.72								
24.5	1.08									
27.5	.90									
30	.70									

TABLE XVI

Lines of Constant $\frac{q-q_s}{q_o-q_s}$

Minimum Value, Pulsating Flow

X/D \ Y/D =	.04	.1	.2	.3	.4	.5	.6	.7	.8	.9
0					.48	.43	.38	.33	.28	.21
3	.56	.53	.51	.48	.45	.42	.35	.29	.25	.15
5	.51	.44	.40	.36	.31	.27	.24	.20	.12	
9	.52	.45	.36	.27	.20	.12				
12	.72	.50	.30	.10						
21	1.14	.52								
24.5	1.33	.40								
27.5	1.57									
30	1.60									

TABLE XVII

Lines of Constant $\frac{q-q_s}{q_o-q_s}$

Intermediate Value, Pulsating Flow

$\frac{x}{D}$ \ $\frac{y}{D}$	.0	.04	.1	.2	.3	.4	.5	.6	.7	.8	.9
0						.48	.44	.40	.35	.30	.19
3	.55	.60	.53	.49	.46	.42	.40	.35	.30	.26	.14
5	.56	.50	.48	.42	.38	.34	.29	.25	.20	.13	
9	.59	.51	.44	.36	.29	.21	.14				
12	.93	.75	.59	.39	.20						
21	1.35	1.10	.28								
24.5	1.55	.93									
27.5	1.66	1.15									
30	1.73	.88									

TABLE XVIII

Lines of Constant $\frac{q-q_s}{q_o-q_s}$

Intermediate Value, Steady Flow

$\frac{X}{D}$ \ $\frac{Y}{D}$=	.016	.1	.2	.3	.4	.5	.6	.7	.8	.9
0					.48	.42	.38	.32	.29	.22
3	.58	.52	.47	.43	.39	.35	.32	.27	.23	.14
5	.67	.58	.52	.45	.39	.32	.25	.17	.11	
9	.87	.62	.48	.39	.30	.21				
12	1.0	.54	.40	.24						
21	1.19									
24.5	1.26									
27.5	1.35									
30	1.4									

TABLE XIX

Lines of Constant $\frac{q-q_s}{q_o-q_s}$

Maximum Value, Steady Flow

$\frac{X}{D}$ \ $\frac{Y}{D}=$	.02	.1	.2	.3	.4	.5	.6	.7	.8	.9
0					.45	.40	.35	.31	.26	.21
3	.58	.50	.45	.42	.39	.35	.31	.27	.23	.18
5	.64	.60	.52	.45	.39	.33	.25	.18		
9	.93	.63	.52	.42	.32	.10				
12	1.02	.66	.43	.23						
21	1.06	.24								
24.5	1.13									
27.5	0.96									
30	0.80									

TABLE XX

CENTERLINE VALUES OF VELOCITY

(a) Steady Flow, intermediate value

$\frac{x}{D}$	$q-q_s$	q_o-q_s	$\frac{q_s}{q_o-q_s}$	$\frac{u-u_s}{u_o-u_s}$
0	9.0	9.0	1.0	1.0
3	8.3	9.0	.925	.963
5	7.9	9.0	.880	.940
9	5.2	9.0	.580	.762
12	3.5	9.0	.390	.625
21	1.0	9.0	.116	.340
24.5	0.8	9.0	.089	.298
27.5	0.55	9.0	.061	.247
30	0.50	9.0	.055	.234

(b) Pulsed Flow, intermediate value

$\frac{x}{D}$	$q-q_s$	q_o-q_s	$\frac{q_s}{q_o-q_s}$	$\frac{u-u_s}{u_o-u_s}$
0	8.05	8.05	1.0	1.0
3	7.80	8.05	.970	.985
5	7.00	8.05	.870	.935
9	4.70	8.05	.585	.765
12	3.00	8.05	.370	.610
21	0.85	8.05	.105	.324
24.5	0.80	8.05	.099	.310
27.5	0.50	8.05	.062	.249
30	0.40	8.05	.050	.224

TABLE XXI

NORMALIZED VELOCITY PROFILES

$$\frac{x}{D} = 12$$

(a) Steady Flow, Intermediate Value: $\frac{r_m}{r_o} = 0.49$, $r_o = 1.1$

$\frac{y}{D}$	q	$q-q_s$	$\frac{q-q_s}{q_o-q_s}$	$\frac{u-u_s}{u_o-u_s}$	$\frac{r}{r_m}$
0	5.9	3.5	1.0	1.0	0
0.1	5.9	3.5	1.0	1.0	0.184
0.2	5.4	3.0	0.855	0.925	0.37
0.3	4.6	2.2	0.63	0.795	0.55
0.4	4.2	1.8	0.515	0.718	0.73
0.5	3.5	1.1	0.315	0.56	0.92
0.6	3.0	0.6	0.171	0.413	1.13
0.7					
0.8	2.7	0.3	0.086	0.293	1.49
0.9	2.6	0.2	0.057	0.239	1.67
1.0	2.5	0.1	0.0285	0.169	1.86
1.1	2.4	0	0		2.04

(b) Pulsed Flow: $\frac{r_m}{r_o} = 0.575$, $r_o = 1.1$

0	6.35	3.15	1	1	0
0.1	6.10	2.90	0.923	0.96	0.159
0.2	5.9	2.7	0.855	0.925	0.317
0.3	5.35	2.15	0.683	0.815	0.475
0.5	4.6	1.4	0.445	0.666	0.790
0.7	3.75	0.55	0.175	0.418	1.10
0.9	3.50	0.30	0.095	0.308	1.42
1.1	3.20	0	0	0	1.74

TABLE XXII

NORMALIZED VELOCITY PROFILES

$\frac{x}{D} = 21$

(a) Steady Flow, Intermediate Value; $\frac{r_m}{r_o} = 0.68$, $r_o = 1.3$

$\frac{y}{D}$	q	$q-q_s$	$\frac{q-q_s}{q_o-q_s}$	$\frac{u-u_s}{u_o-u_s}$	$\frac{r}{r_m}$
0	3.4	1.0	1.0	1.0	0.0
.1	3.4	1.0	1.0	1.0	0.11
.2	3.35	0.95	0.95	0.975	0.23
.3	3.2	0.80	0.80	0.895	0.34
.4	3.1	0.70	0.70	0.835	0.46
.5	3.0	0.60	0.60	0.775	0.57
.6	2.9	0.50	0.50	0.705	0.68
.8	2.7	0.30	0.30	0.55	0.91
1.0	2.6	0.20	0.20	0.45	1.14
1.1	2.55	0.15	0.15	0.39	1.25
1.2	2.50	0.10	0.10	0.31	1.35
1.3	2.4	0	0	0	1.47

(b) Pulsed Flow; $\frac{r_m}{r_o} = 0.68$, $r_o = 1.5$

0	4.20	0.95	1	1	0
0.8	3.85	0.50	0.527	0.725	0.69
1.2	3.55	0.20	0.211	0.460	1.04
1.3	3.45	0.05	0.0527	0.229	1.125
1.5	3.35	0	0	0	1.3

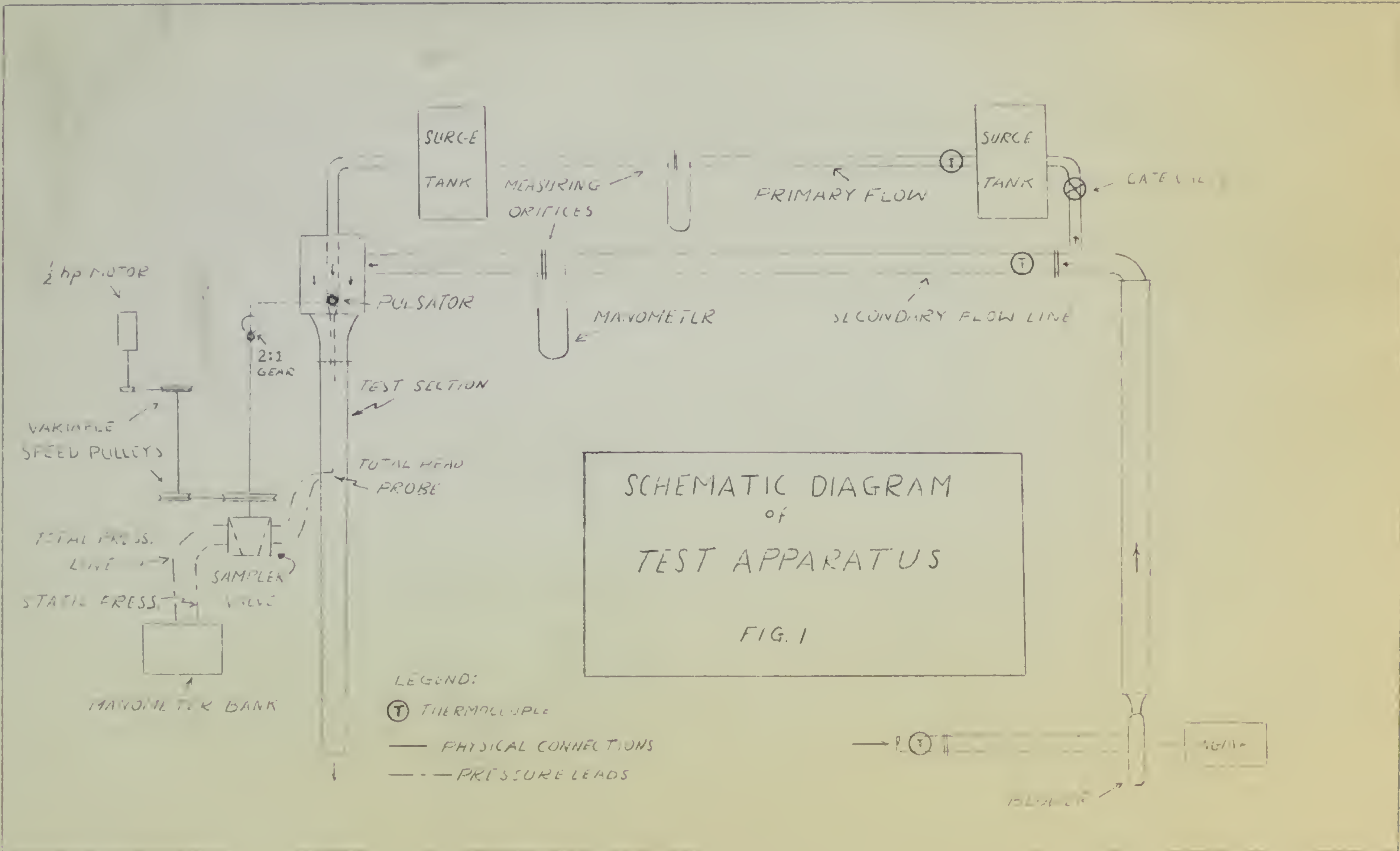

SCHEMATIC DIAGRAM
of
TEST APPARATUS

FIG. 1

Fig. 2-a Control panel for engine operation

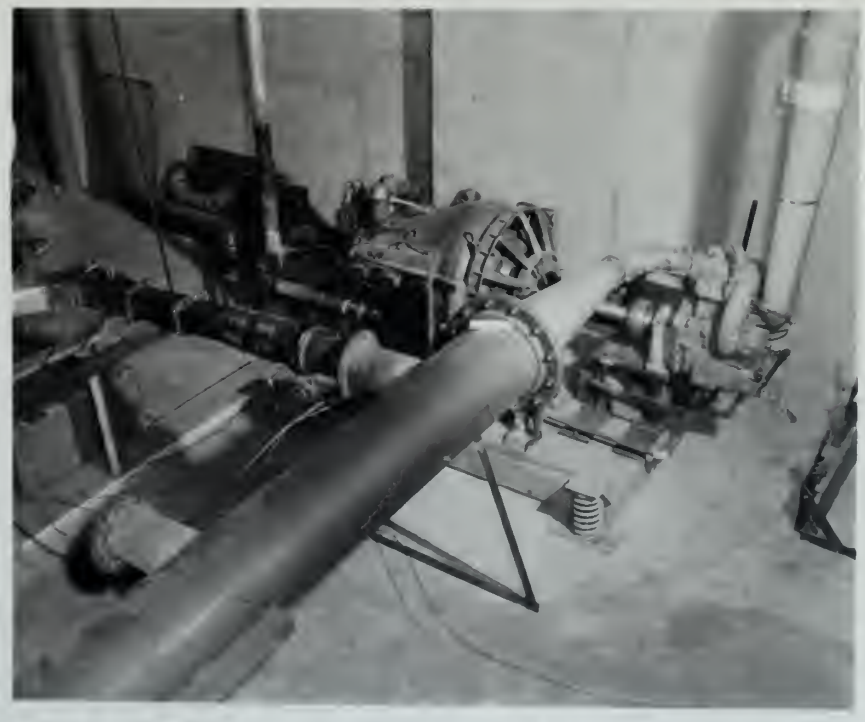

Fig. 2-b Engine, blower, and manifold

(The test set-up shown is not part of this experiment)

Fig. 2-c Sampler valve, test section, and pressure leads

[illegible]

Fig. 2-e Stilling chamber; pulsator in primary flow line

Fig. 2-f Area reducers for primary and secondary flow

Fig. 2-g Complete assembly, showing large surge tanks

Fig. 2-h Airflow system from manifold to test section

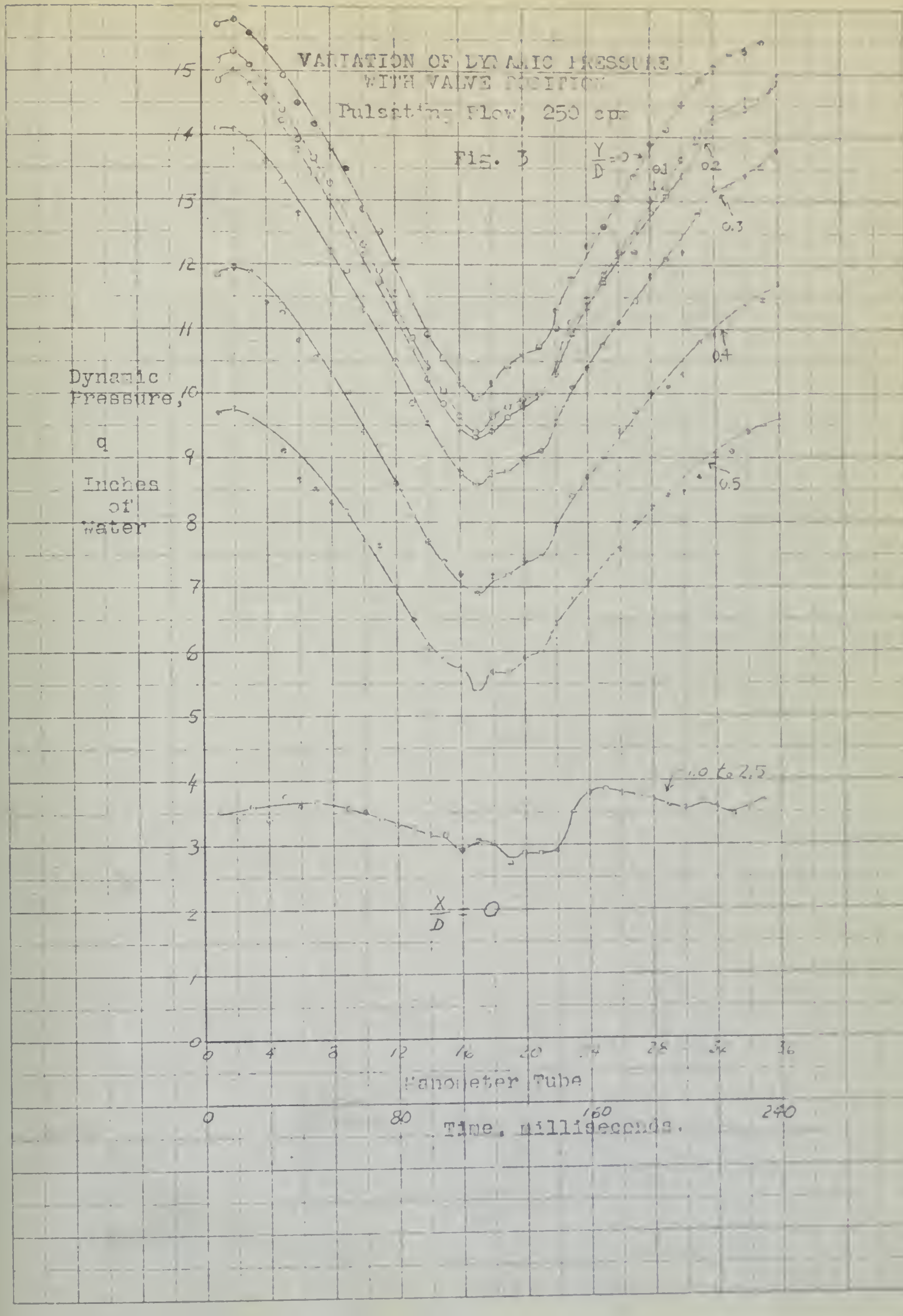
VARIATION OF DYNAMIC PRESSURE
WITH VALVE POSITION
Pulsating Flow, 250 cpm
Fig. 3
Y/D = 0
0.1
0.2
0.3
0.4
0.5
1.0 to 2.5
X/D = 0
Dynamic Pressure,
q
Inches of Water
Manometer Tube
Time, milliseconds.

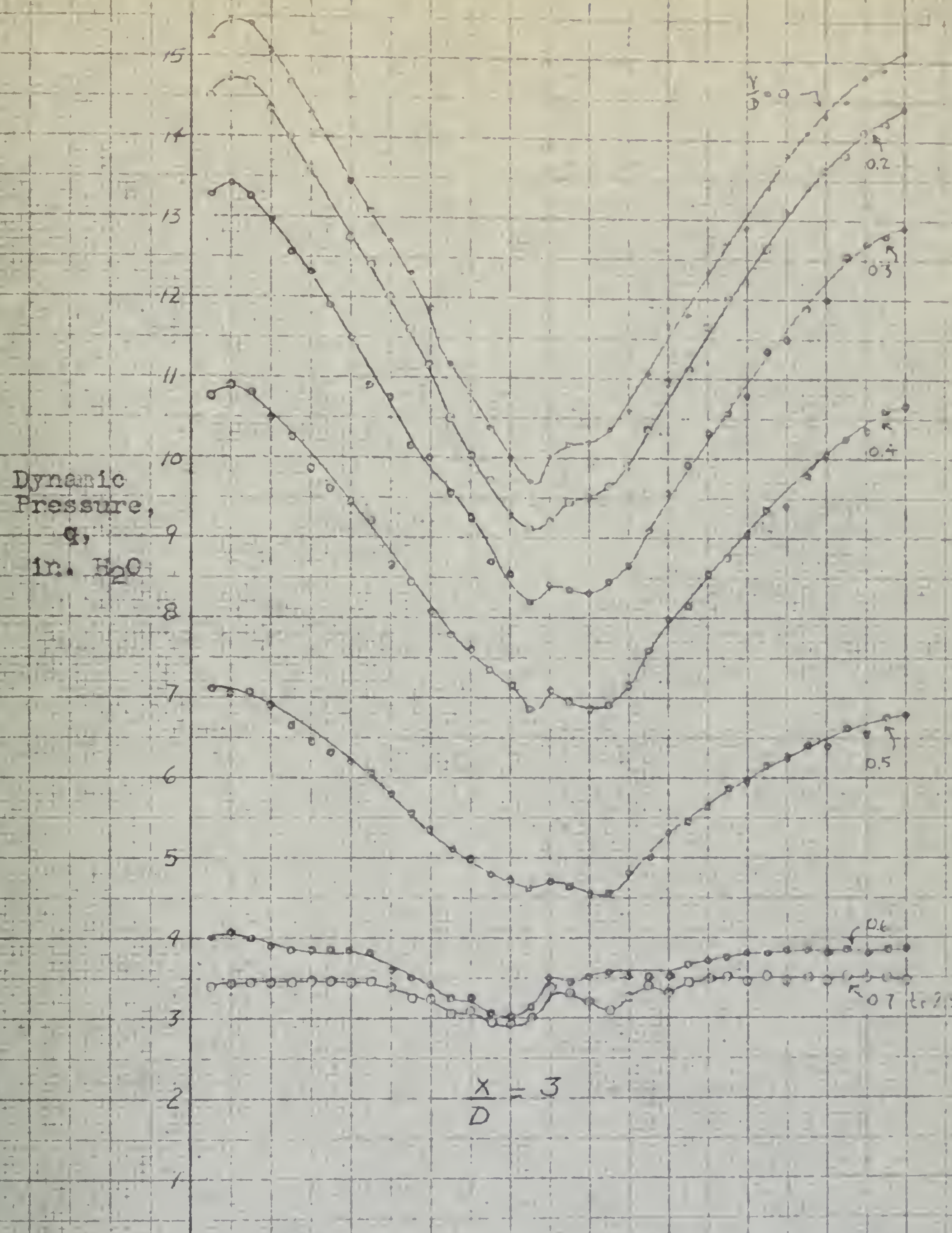

VARIATION OF DYNAMIC PRESSURE
with VALVE POSITION
Pulsating Flow, 250 cpm

Fig. 4

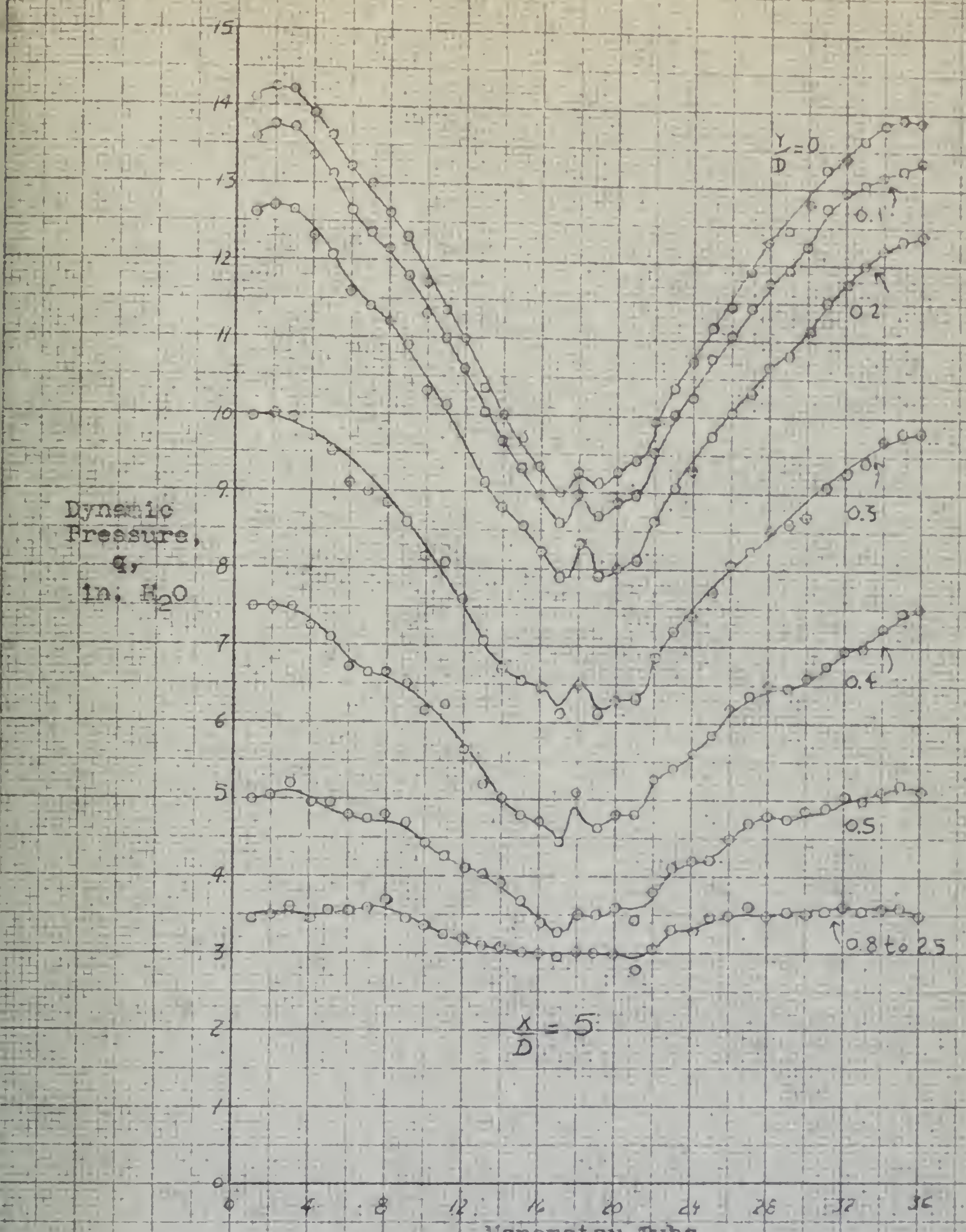

VARIATION OF DYNAMIC PRESSURE WITH VALVE POSITION

Pulsating Flow, 250 cpm

Fig. 5

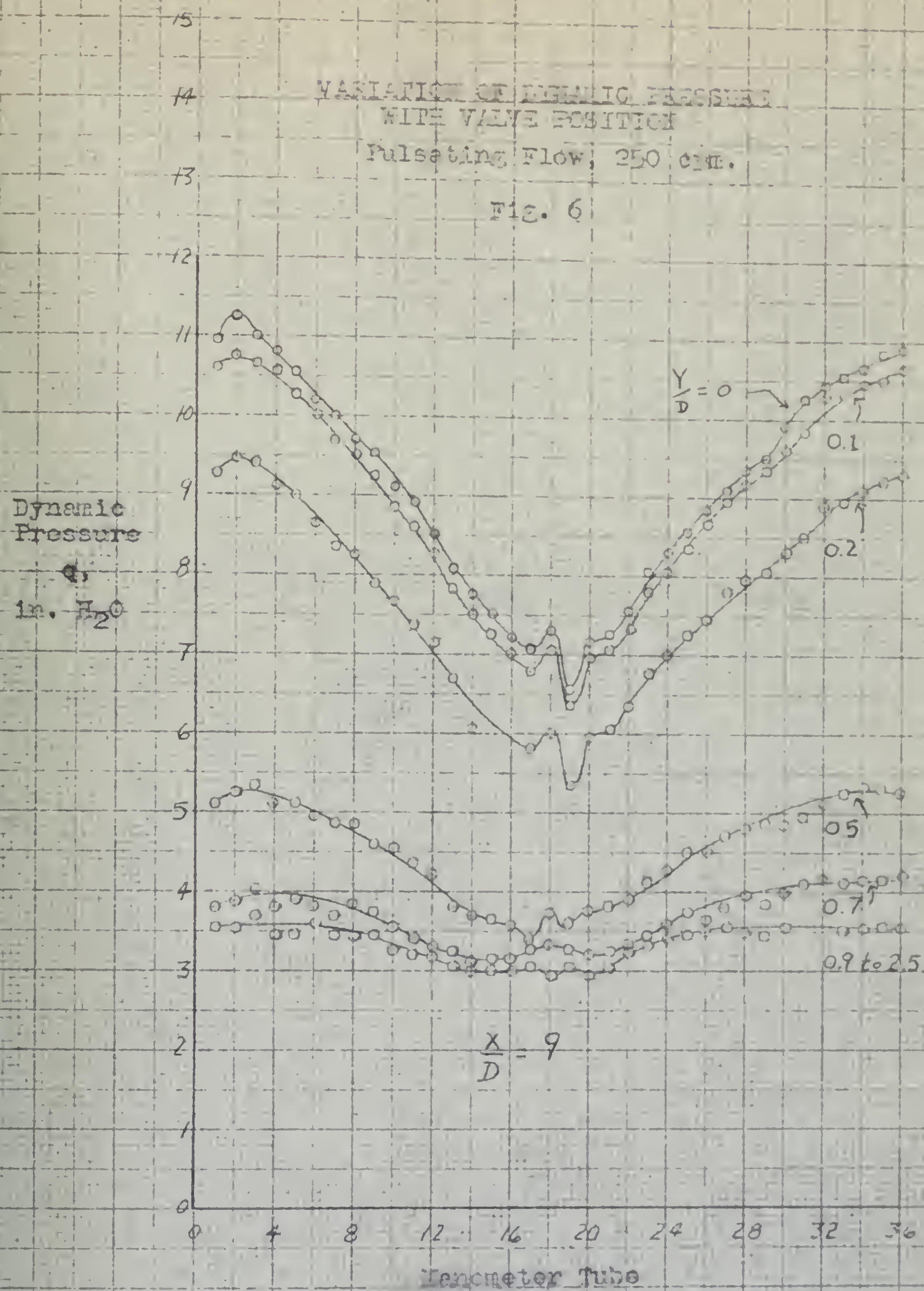

VARIATION OF DYNAMIC PRESSURE WITH VALVE POSITION

Pulsating Flow, 250 cfm.

Fig. 6

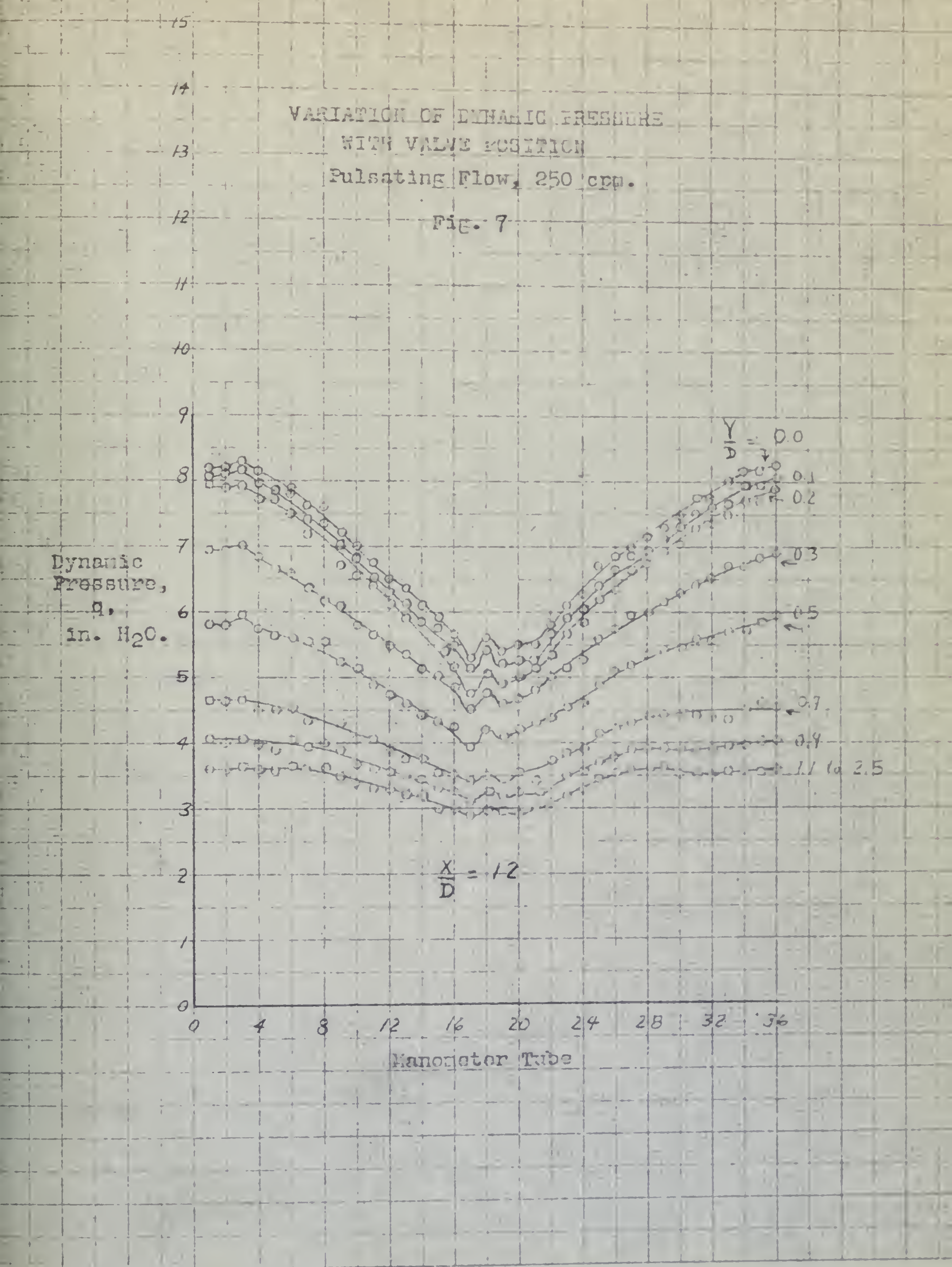
VARIATION OF DYNAMIC PRESSURE
WITH VALVE POSITION
Pulsating Flow, 250 cpm.
Fig. 7
Dynamic Pressure, q, in. H_2O.
Manometer Tube
Y/D = 0.0
0.1
0.2
0.3
0.5
0.7
0.9
1.1 to 2.5
X/D = 12
0
1
2
3
4
5
6
7
8
9
10
11
12
13
14
15
0
4
8
12
16
20
24
28
32
36

VARIATION OF DYNAMIC PRESSURE
WITH VALVE POSITION

Pulsating Flow, 250 cpm.

Fig. 8

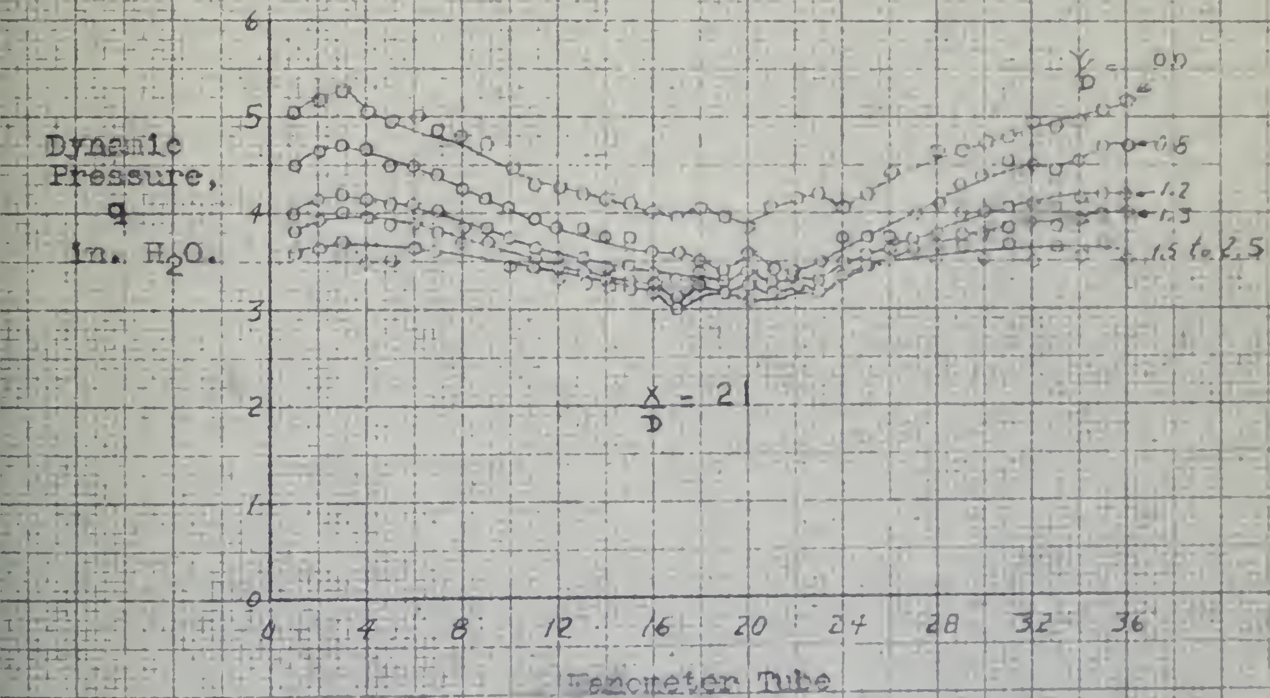

VARIATION OF DYNAMIC PRESSURE
WITH VALVE POSITION
Pulsating Flow, 250 cpm.

Fig. 9

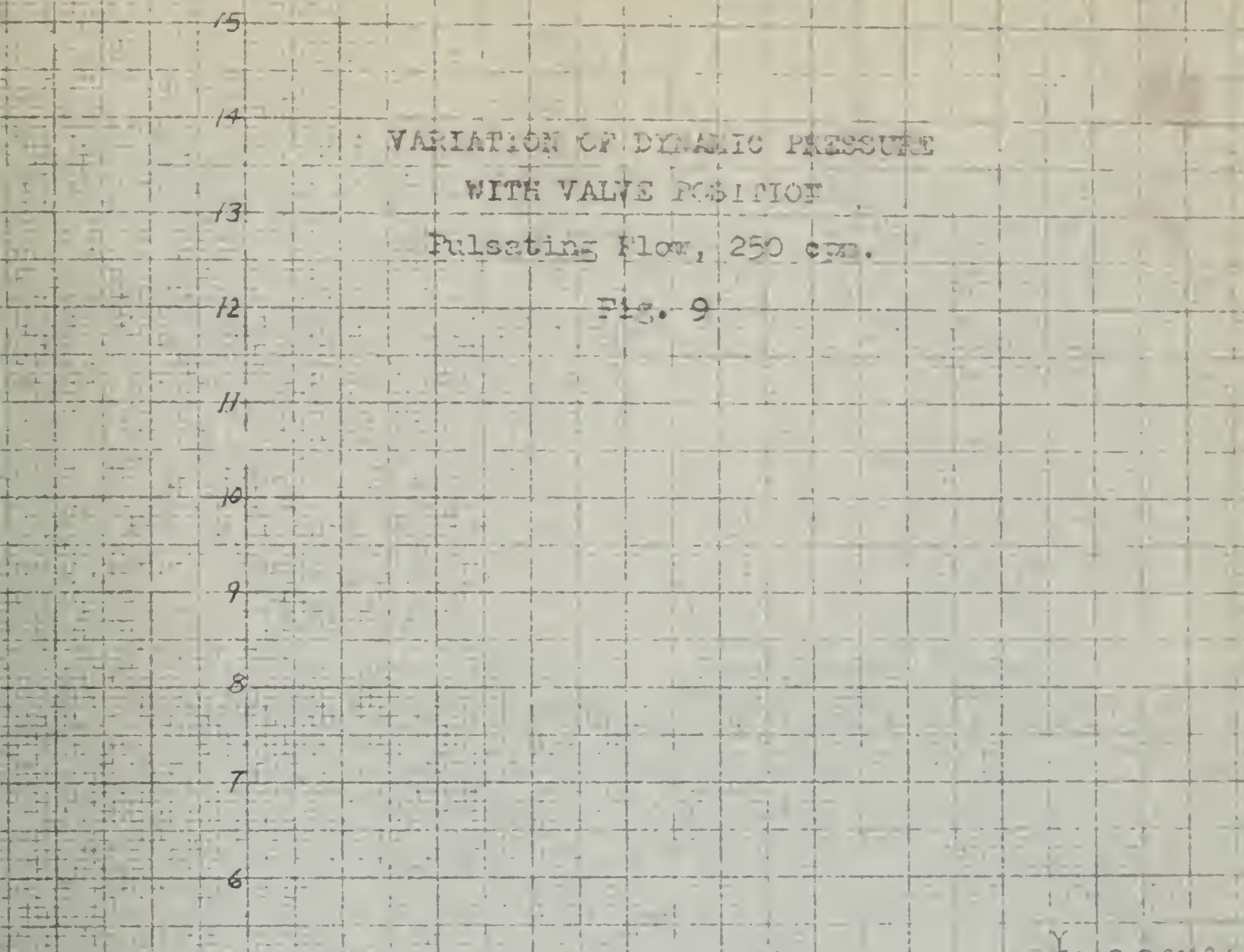

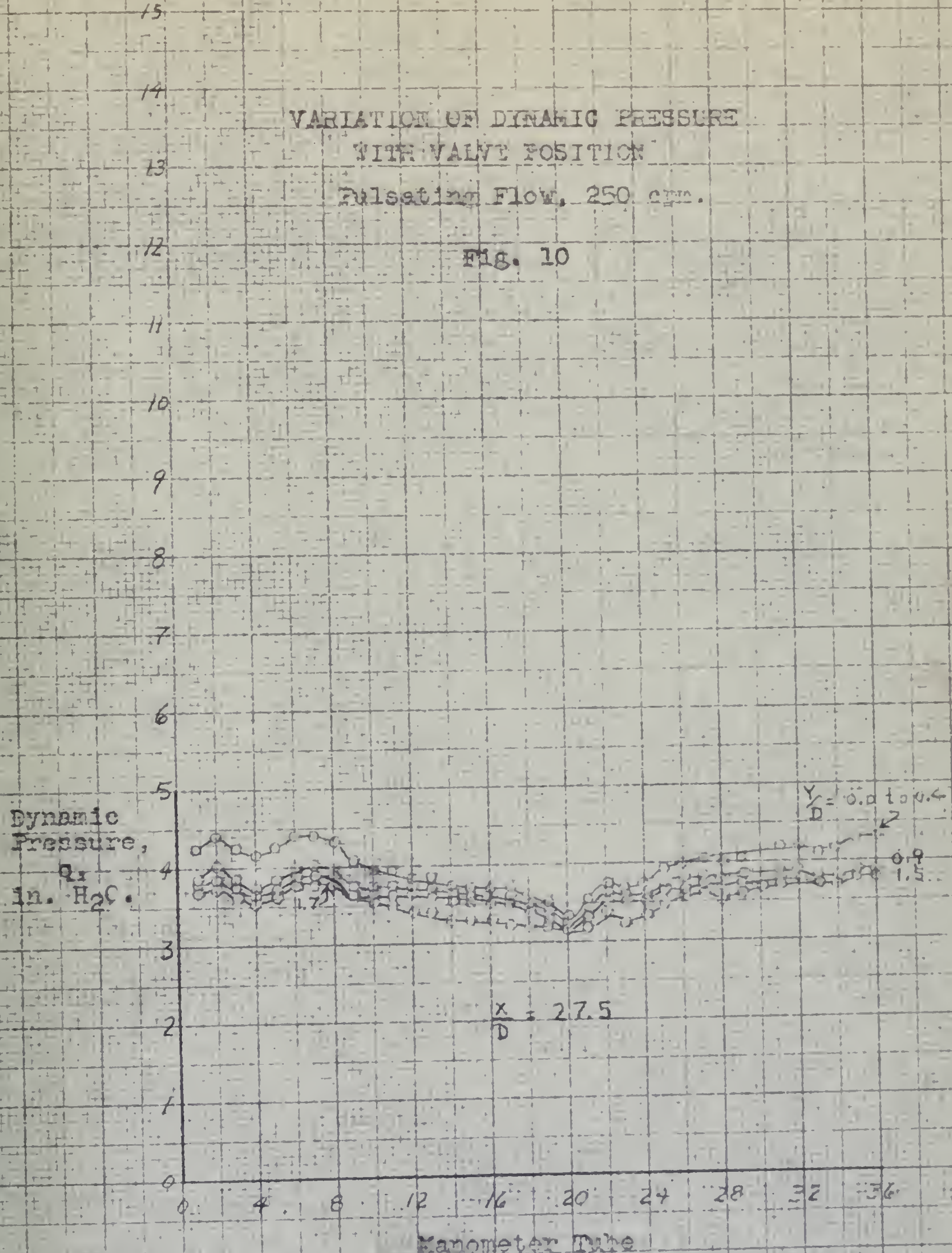

VARIATION OF DYNAMIC PRESSURE WITH VALVE POSITION

Pulsating Flow, 250 cpm.

Fig. 10

VARIATION OF DYNAMIC PRESSURE
WITH VALVE POSITION
Pulsating Flow, 250 cpm.

Fig. 11

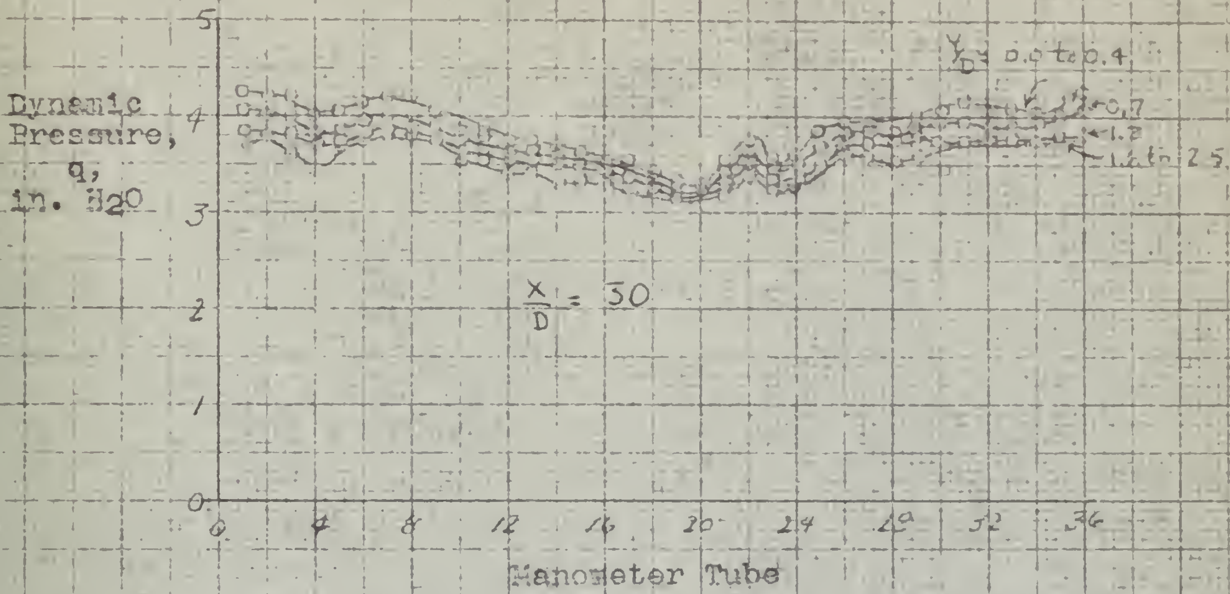

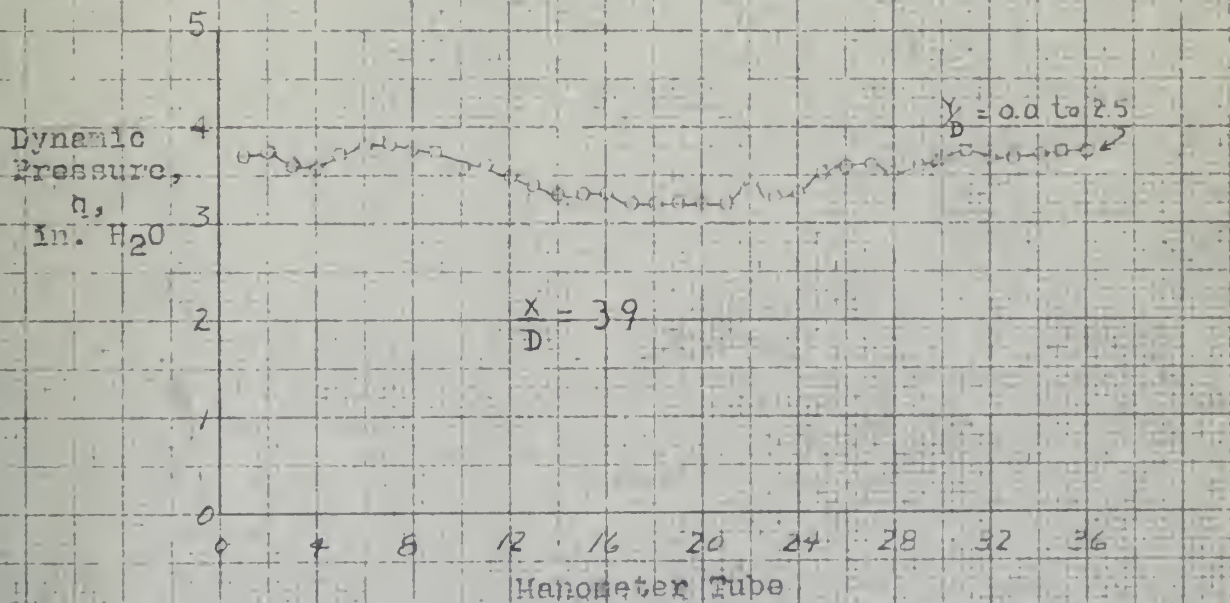

Fig. 12

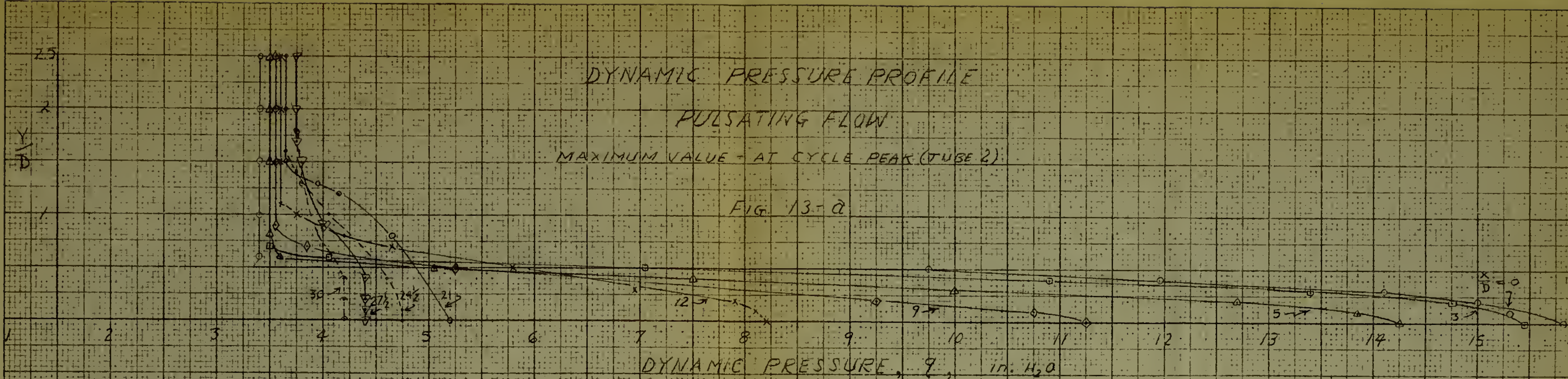

FIG. 13-a

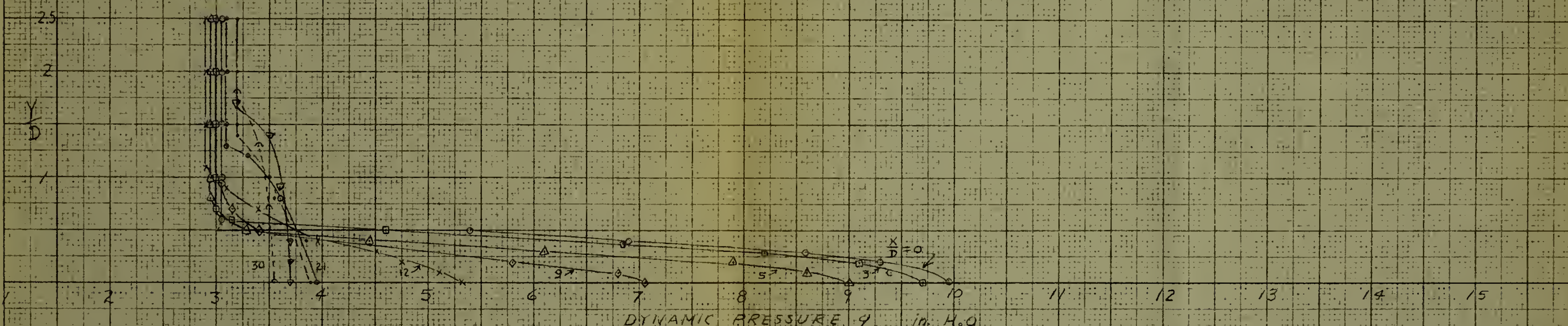

MINIMUM VALUE - AT CYCLE TROUGH (TUBE 17)

FIG. 13-b

Y = Distance From Nozzle Centerline
D = Nozzle Diameter
Air flow at 136°F, P_s = 14.45 psi

DYNAMIC PRESSURE PROFILE

PULSATING FLOW

INTERMEDIATE VALVE - (TUBE 13)

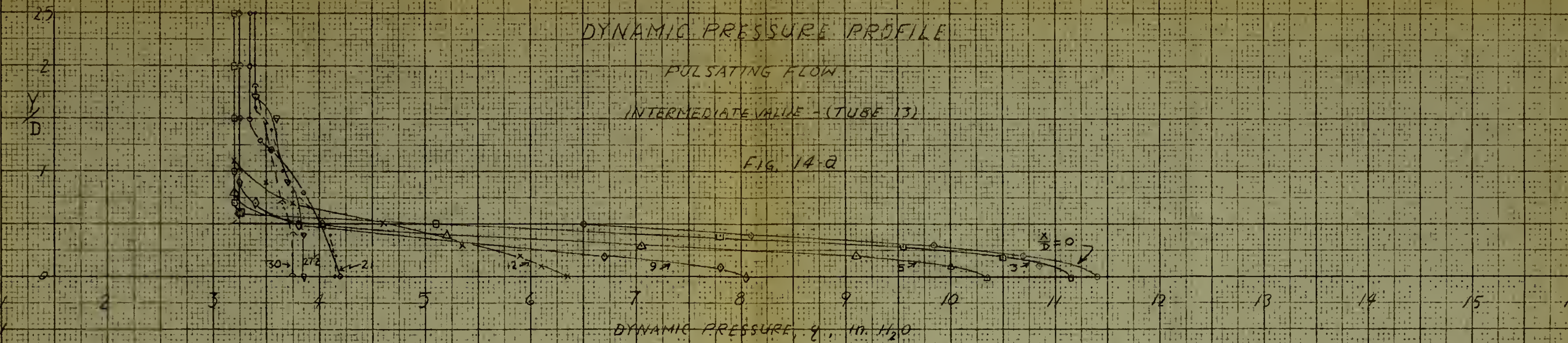

FIG. 14-a

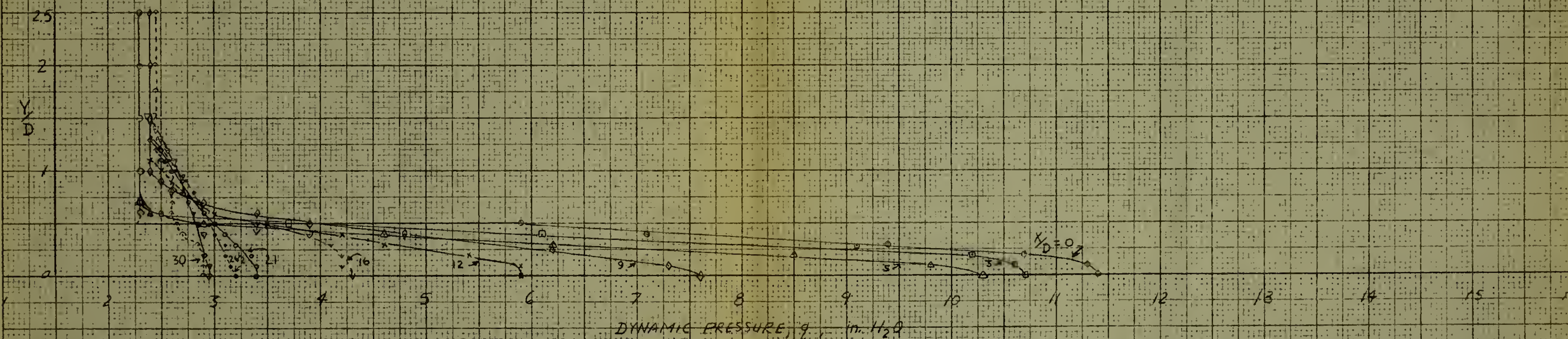

STEADY FLOW

(MASS RATE OF PRIMARY FLOW SAME AS FOR PULSED FLOW)

FIG. 14-b

Y = Distance From Nozzle Centerline.

D = Nozzle Diameter

Air Flow at 136°F; P_s = 14.45 psi.

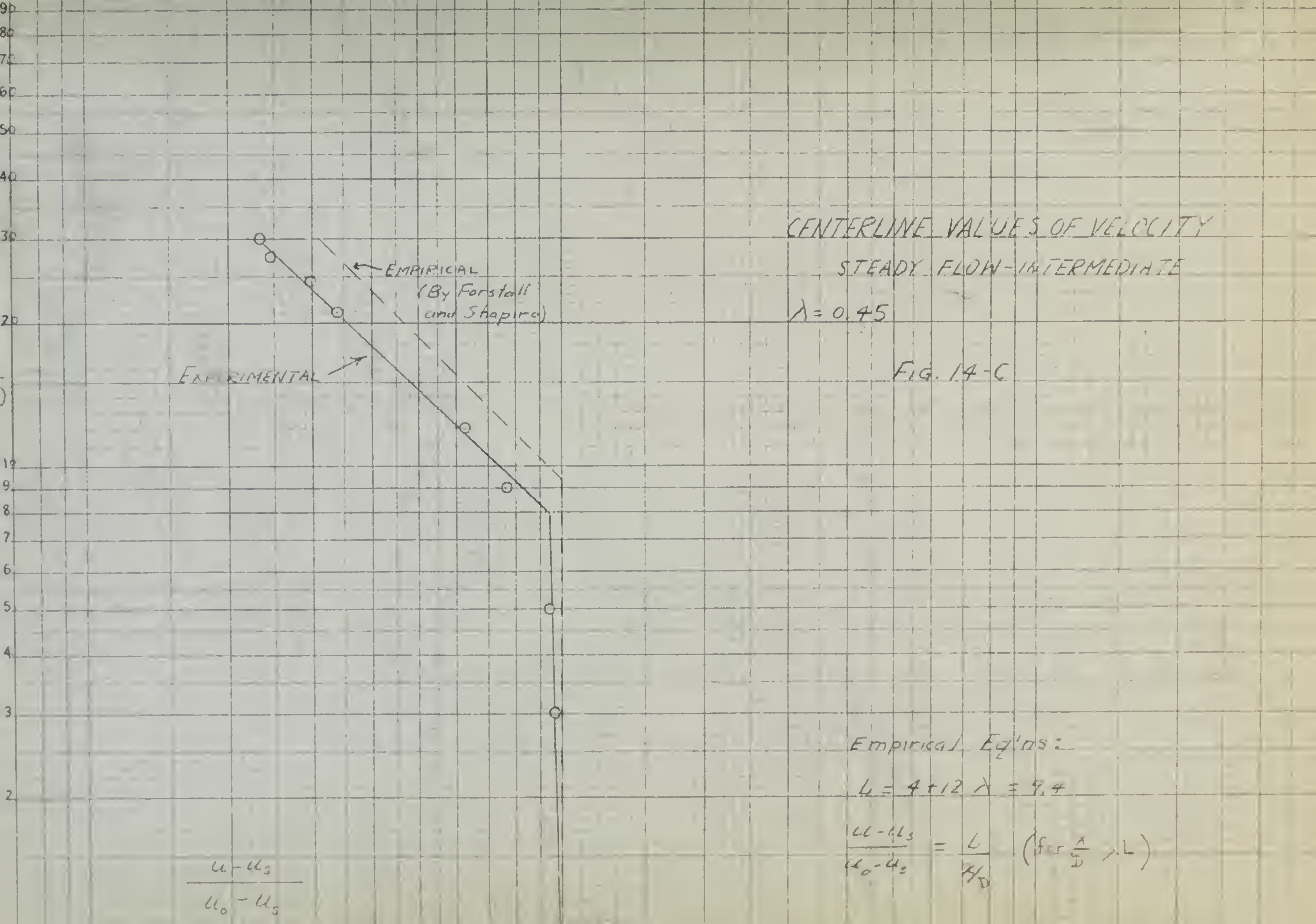
CENTERLINE VALUES OF VELOCITY
STEADY FLOW-INTERMEDIATE
$\lambda = 0.45$
FIG. 14-C
EMPIRICAL
(By Forstall and Shapiro)
EXPERIMENTAL
Empirical Eq'ns:
$L = 4 + 12\lambda = 9.4$
$\frac{u-u_s}{u_o-u_s} = \frac{L}{x/D}$ (for $\frac{x}{D} > L$)
$\frac{u-u_s}{u_o-u_s}$
90
80
70
60
50
40
30
20
10
9
8
7
6
5
4
3
2

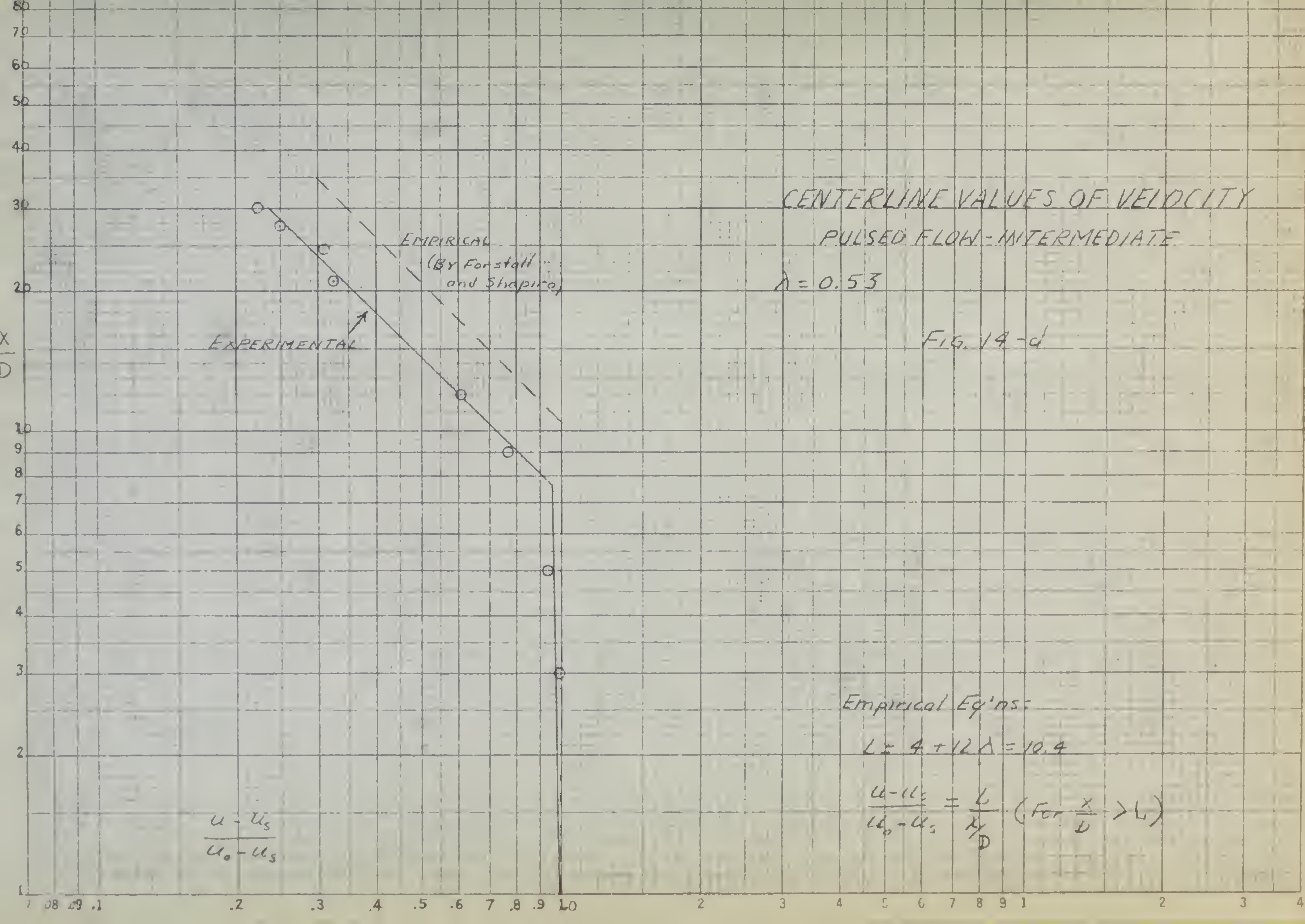
CENTERLINE VALUES OF VELOCITY
PULSED FLOW - INTERMEDIATE
$\lambda = 0.53$
FIG. 14-d
EMPIRICAL
(By Forstall and Shapiro)
EXPERIMENTAL
$\frac{x}{D}$
$\frac{u - u_s}{u_0 - u_s}$
Empirical Eq'ns:
$L = 4 + 12\lambda = 10.4$
$\frac{u - u_s}{u_0 - u_s} = \frac{L}{x/D}$ (For $\frac{x}{D} > L$)

NORMALIZED VELOCITY PROFILES

FIG 14-E

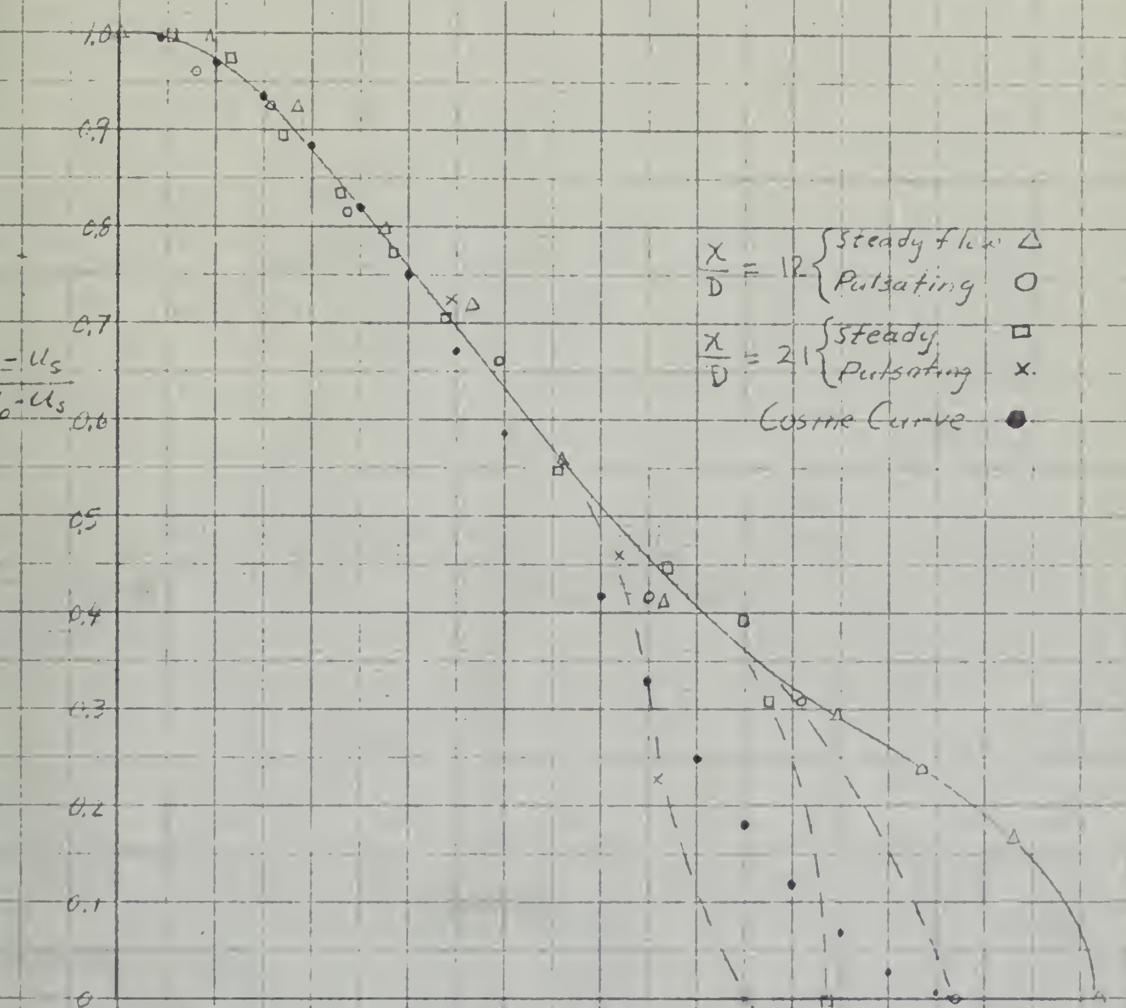

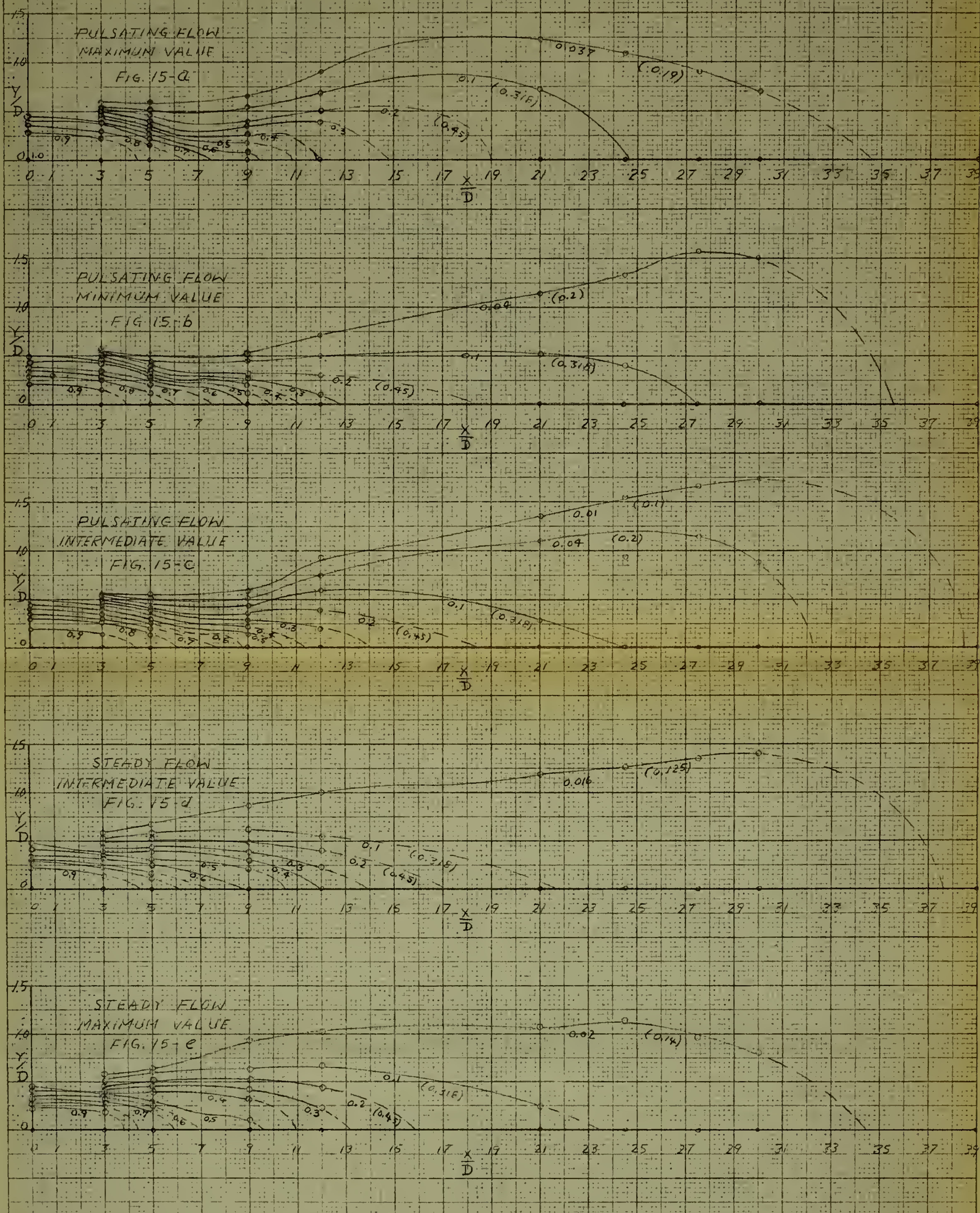

AIRJET MIXING REGIONS

PULSATING AND STEADY

SHOWN BY LINES OF CONSTANT $\frac{q-q_s}{q_o-q_s}$

(VALUES OF $\frac{u-u_s}{u_o-u_s}$ ARE IN PARENTHESES)

FIG. 15